Quaternary Science Reviews 256 (2021) 106813

Contents lists available at ScienceDirect

Quaternary Science Reviews

journal homepage: www.elsevier.com/locate/quascirev

Spatial variation of hydroclimate in north-eastern North America during the last millennium

Helen Mackay [a, *], Matthew J. Amesbury [b], Pete G. Langdon [c], Dan J. Charman [b], Gabriel Magnan [d], Simon van Bellen [d], Michelle Garneau [d], Rupert Bainbridge [e], Paul D.M. Hughes [c]

[a] Department of Geography, Durham University, Durham, UK
[b] Geography, College of Life and Environmental Sciences, University of Exeter, UK
[c] Geography and Environmental Sciences, University of Southampton, UK
[d] Geotop, Université du Québec à Montréal, Canada
[e] Geography, Politics and Sociology, Newcastle University, UK

ARTICLE INFO

Article history:
Received 4 September 2020
Received in revised form
15 January 2021
Accepted 16 January 2021
Available online 12 February 2021

Handling Editor: I Hendry

Keywords:
North America
Peatlands
Hydroclimate
Testate amoebae
Palaeoclimate
Late Holocene
Little Ice Age
Medieval Climate Anomaly

ABSTRACT

Climatic expressions of the Medieval Climate Anomaly (MCA) and the Little Ice Age (LIA) vary regionally, with reconstructions often depicting complex spatial patterns of temperature and precipitation change. The characterisation of these spatial patterns helps advance understanding of hydroclimate variability and associated responses of human and natural systems to climate change. Many regions, including north-eastern North America, still lack well-resolved records of past hydrological change. Here, we reconstruct hydroclimatic change over the past millennium using testate amoeba-inferred peatland water table depth reconstructions obtained from fifteen peatlands across Maine, Nova Scotia, Newfoundland and Québec. Spatial comparisons of reconstructed water table depths reveal complex hydroclimatic patterns that varied over the last millennium. The records suggest a spatially divergent pattern across the region during the Medieval Climate Anomaly and the Little Ice Age. Southern peatlands were wetter during the Medieval Climate Anomaly, whilst northern and more continental sites were drier. There is no evidence at the multi-decadal sampling resolution of this study to indicate that Medieval mega-droughts recorded in the west and continental interior of North America extended to these peatlands in the north-east of the continent. Reconstructed Little Ice Age hydroclimate change was spatially variable rather than displaying a clear directional shift or latitudinal trends, which may relate to local temporary permafrost aggradation in northern sites, and reconstructed characteristics of some dry periods during the Little Ice Age are comparable with those reconstructed during the Medieval Climate Anomaly. The spatial hydroclimatic trends identified here suggest that over the last millennium, peatland moisture balance in north-eastern North America has been influenced by changes in the Polar Jet Stream, storm activities and sea surface temperatures in the North Atlantic as well as internal peatland dynamics.

1. Introduction

The last millennium is a key focus for palaeoclimate reconstruction and climate modelling because environmental boundary conditions are broadly comparable with the present day and detailed climate reconstructions can be obtained from well-resolved proxy data with robust chronological control. However, despite its critical effect on human and natural systems, understanding of hydroclimate variability over the Common Era is limited, in part due to a lack of spatially resolved palaeoclimatic data (Steiger et al., 2018). Within the last millennium, the three most prominent periods of widespread Northern Hemisphere climatic change are: the Medieval Climate Anomaly (MCA), associated with increased temperature *ca.* 950–1250 CE (Jansen et al., 2007; Mann et al., 2008, 2009); the Little Ice Age (LIA), marked with cooler climate conditions *ca.*1400–1700 CE (Jansen et al., 2007; Mann et al., 2008, 2009) and recent warming (since 1850 CE). The MCA is often considered a partial analogue for current climate

* Corresponding author.
E-mail address: helen.mackay@durham.ac.uk (H. Mackay).

https://doi.org/10.1016/j.quascirev.2021.106813

change because mean surface air temperatures, if not rates of change, were comparable with early 21st century warming. For example, reconstructed MCA mean surface temperatures in the North Atlantic region were 0.9–1.4 °C above the 1961–1990 reference period (Mann et al., 2009). Conversely, the LIA was associated with mean Northern Hemisphere surface temperature decreases of *ca.* 0.5 °C (Mann et al., 2009), which strongly impacted natural ecosystems and disrupted human society (Lamb, 1977; Grove 1988). The MCA and LIA predate the Industrial Revolution; therefore, they act as excellent case studies to further understand natural ecosystem functioning and climate variability.

Both the MCA and LIA have been described as global events (e.g. Mann et al., 2009; Graham et al., 2010; Lüning et al., 2017), but the timing and extent of these periods, as well as their hydroclimatic effects, are regionally variable. For example, whilst extensive MCA droughts have been reconstructed across the Western and Midwestern US (e.g. Cook et al., 2010), the eastward extent of these events remains unclear, partly due to the lack of well-constrained late Holocene hydroclimatic records developed from north-eastern US and Atlantic Canada (Shuman et al., 2018). The timing of the LIA in north-eastern North America is also debated since tree-ring reconstructions from northern boreal Quebec demonstrate that cooling began later, in 1450 CE, and that the coolest phase occurred during the 19th century in many regions (Naulier et al., 2015). The majority of existing palaeoclimatic records from north-eastern North America have either; 1) a longer temporal focus (e.g. Newby et al., 2014; Neil and Gajewski, 2017; Blundell et al., 2018), with relatively low temporal resolution for the last millennium, or 2) have been restricted to the latitudinal extremities of the region in Newfoundland (Hughes et al., 2006; Daley et al., 2016) and Maine (Nichols and Huang., 2012; Clifford and Booth, 2013, 2015). In order to improve our understanding of hydroclimate variability related to past climate change, the spatial coverage of palaeoclimate reconstructions along the eastern seaboard of the North Atlantic must be increased, particularly for the Medieval period (Neukom et al., 2018).

Ombrotrophic (rain-fed) peatlands are sensitive to climate change, with records of past variability in peatland water table depth (WTD) representing the prevailing balance between precipitation and evapotranspiration across the growing season (Charman et al., 2009). The responsiveness of these ecosystems to Holocene climate variability throughout north-eastern US and Atlantic Canada has been clearly demonstrated (e.g. Hughes et al., 2006; Nichols and Huang, 2012; Clifford and Booth, 2013; Clifford and Booth, 2015; Blundell et al., 2018). In addition, comparisons of regional records facilitate the distinction of hydrological changes driven by allogenic forcing (i.e. climate) from autogenic changes driven by internal peatland dynamics and ecohydrological feedback mechanisms (Belyea, 2009; Swindles et al., 2012; Morris et al., 2015). Whilst the characteristics of climatically-driven hydrological responses may vary between peatland sites, broadly synchronous changes in multiple sites can be attributed to climatic control (e.g. Magnan et al., 2018; Van Bellen et al., 2018; Piilo et al., 2019).

The current climate of the north-eastern US and Atlantic Canada region is influenced by cold dry Arctic air masses, mild dry Pacific Westerlies, warm moist tropical maritime air masses and oceanic interactions between the Labrador Current and the Gulf Stream. The combined influence of these climatic controls generates longitudinal oceanic to continental, as well as latitudinal terrestrial temperature and precipitation gradients (Fig. 1). Whilst broad-scale climate variability is overlain by smaller scale local variability, east coast temperatures generally decrease with increasing latitude and, whilst latitudinal precipitation gradients have a more complex spatial pattern, generally precipitation decreases from southern boreal Québec northward into the high boreal, subarctic and Arctic. Projections of future annual temperature changes in north-eastern North America suggest a 2–3 °C increase by 2050 (Bruce, 2011; Wuebbles et al., 2017), with greater seasonal temperature increases projected for summer months compared with winter months (Wuebbles et al., 2017). Summer (June, July, August; JJA) precipitation-change projections over the same time period contain more complex spatial patterns, with median decreases of up to 10% in northern Nova Scotia and southern Newfoundland and increases of up to 10% in Maine and Québec (Wuebbles et al., 2017).

The aim of this study is to improve understanding of hydroclimate variability during the last millennium in north-eastern US and Atlantic Canada by addressing the following questions: (1) Do the multi-decadal Medieval dry periods detected in the Western and Midwestern US extend to north-eastern North America? (2)

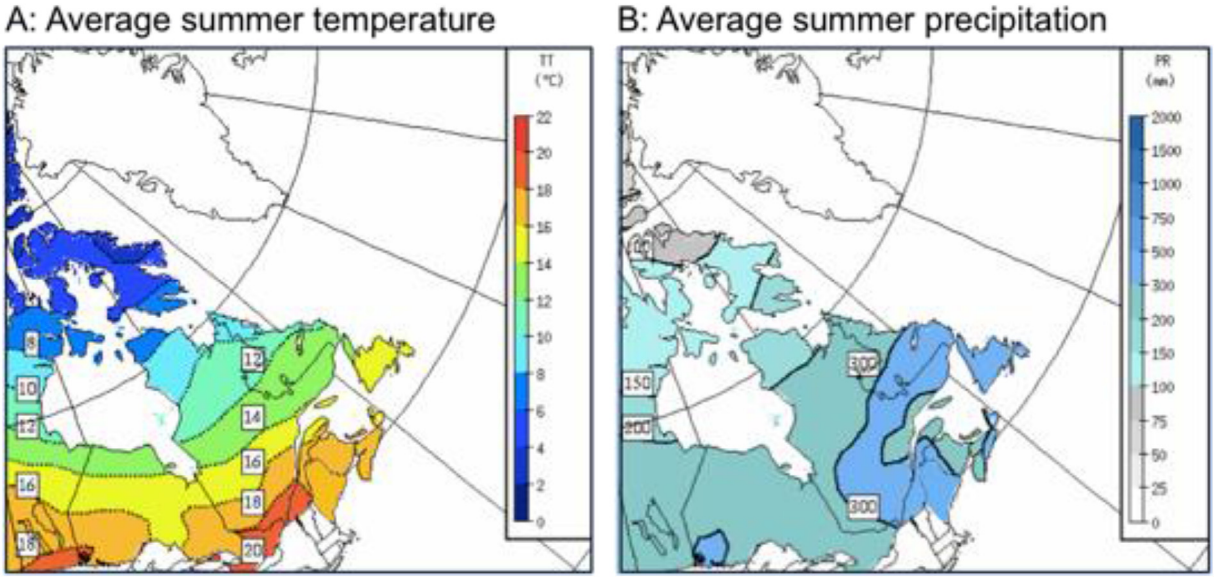

Fig. 1. Average summer (June–August) temperature (A) and precipitation (B) gradients across north-eastern North America from 1981 to 2010 (adapted from Environment Canada (2010) and NOAA National Centres for Environmental Information (2018)).

What regional patterns in MCA and LIA climate change can be detected? (3) Do these regional patterns of climate change provide any insight into dominant climate forcing mechanisms? To address these questions, this study reconstructs summer hydroclimate variability over the past 1250 years from fifteen ombrotrophic peatlands across Québec, Newfoundland and Nova Scotia, Canada and Maine, USA.

2. Methods

2.1. Study sites

The fifteen study sites are ombrotrophic peatlands located in Québec, Newfoundland, Nova Scotia and Maine (Fig. 2, Table 1). These study sites are located across two Köppen-Geiger climate classification zones based on differences in summer temperatures (Kottek et al., 2006): all study sites in Québec and the most northerly site in Newfoundland (Burnt Village Bog) are located in zone Dfc (snow, fully humid, cool summers and cold winters), whilst the other more southerly sites in Newfoundland (Nordan's and Jeffrey's) and those in Nova Scotia and Maine are located in zone Dfb (snow, fully humid, warm summers with threshold temperature $\geq +10$ °C for at least four months) (Table 1).

The seven new records developed for this study were obtained from locations on ombrotrophic peatlands with minimal anthropogenic disturbances and were distributed to address spatial gaps in the availability of late Holocene peatland hydroclimatic reconstructions. Whilst there is also a need for more peatland palaeohydrological reconstructions from other regions of the wider study area, such as southern Quebec, New Brunswick and Maine, this study primarily focused on addressing the data gap from more eastern and northern maritime climate areas of Nova Scotia and Newfoundland. One core from each study site was extracted from a lawn microform near the centre of each bog following the protocol of Barber et al. (1994) using an 11-cm-diameter Russian corer, following a stratigraphic investigation using the Tröels-Smith (1955) system. Cores were stored in PVC tubes, wrapped in plastic film and stored at 4 °C in preparation for analysis and long-term storage.

2.2. Chronologies

Published age-depth models for Burnt Village Bog, Nordan's Pond Bog, Petite Bog, Sidney Bog (Charman et al., 2015), Lac Le

Fig. 2. Location of study sites that are used within this regional data comparison. Burnt Village Bog (BVB), Jeffrey's Bog (JRB), Framboise Bog (FBB), Petite Bog (PTB), Villagedale Bog (VDB) (black; unpublished sites, this study), Sidney Bog (SDY) and Saco Heath (SCH) (grey; unpublished sites, this study, and published testate-amoebae based peatland hydrological reconstructions (Clifford and Booth, 2013; Clifford and Booth, 2015)) and Lac Le Caron (LLC), Mosaik (MOS), Sterne (STE), Baie (BAI), Lebel (LEB), Morts (MOR), Plaine (PLA), Nordan's Pond Bog (NDN) (red; previously published eastern North American testate-amoebae assemblage data (van Bellen et al., 2011; Garneau et al., 2014; Magnan and Garneau, 2014; Hughes et al., 2006)). (For interpretation of the references to colour in this figure legend, the reader is referred to the Web version of this article.)

Table 1
Site data. *No basal age is available for VDB, deepest available radiocarbon date was obtained from 180 cm.

Site name	Location	Latitude	Longitude	Elevation (m asl)	Total peat depth (cm)	Basal age (wmean) (cal yr BP)	Approx. depth 1250 cal yr BP (cm)
Lac Le Caron	James Bay Lowlands Quebec	52.29	−75.84	255	483	7520	106
Mosaik	James Bay Lowlands Quebec	51.98	−75.40	298	297	7070	72
Sterne	James Bay Lowlands Quebec	52.04	−75.17	303	286	7010	84
Baie	St. Lawrence Estuary Quebec	49.10	−68.25	17	456	4215	124
Lebel	St. Lawrence Estuary Quebec	49.11	−68.24	22	575	5820	136
Morts	Gulf of St. Lawrence Quebec	50.26	−63.67	15	286	3245	100
Plaine	Gulf of St. Lawrence Quebec	50.28	−63.54	18	357	7450	52
Burnt Village Bog	Newfoundland	51.13	−55.93	28	546	8555 ± 202	62
Nordan's Pond Bog	Newfoundland	49.16	−53.60	28	720	8855 ± 141	168
Jeffrey's Bog	Newfoundland	48.21	−58.82	52	385	3395 ± 157	146
Framboise Bog	Nova Scotia	45.72	−60.55	90	448	10,120 ± 273	79
Petite Bog	Nova Scotia	45.14	−63.94	50	860	10,925 ± 378	156
Villagedale Bog	Nova Scotia	43.52	−65.53	15	449	*180 cm = 1930 ± 148	117
Sidney Bog	Maine	44.39	−69.79	24	725	7075 ± 266	138
Saco Heath	Maine	43.55	−70.47	44	370	5015 ± 406	137

Caron, Mosaik, Sterne (van Bellen et al., 2011), Baie, Lebel, Morts and Plaine (Magnan and Garneau, 2014), were applied in this study (Fig. A1, Supplementary Information). Updated age-depth models were constructed for Saco Heath, Villagedale Bog, Framboise Bog and Jeffrey's Bog to combine ^{14}C measurements of *Sphagnum* stems with published tephrochronologies for the sites (Mackay et al., 2016, Fig. A2, Supplementary Information). Bayesian age-depth models were constructed using the R package "BACON" (Blaauw and Christen, 2011). Ages are reported as calibrated years before present (cal yr BP), with 0 cal yr BP corresponding to 1950 CE. Four time periods of interest have been selected to focus on climate changes during the MCA and LIA (as defined by Mann et al., 2009) and climatic conditions before and after these time periods, defined here as: pre-MCA (1250-1000 cal yr BP), MCA (1000-750 cal yr BP), LIA (550-250 cal yr BP) and post-LIA (150−0 cal yr BP).

2.3. Testate amoebae and reconstructed water table depths

Testate amoeba analysis is a well-established proxy in peatlands that is well-suited to reconstructing past hydroclimatic variability because species assemblages predominantly respond to changes in peatland surface moisture (e.g. Woodland et al., 1998; Mitchell et al., 2008). Within this study, testate amoeba analysis was completed across all cores at 2−4 cm intervals to equate to approximately 40-year resolution. Testate amoebae were extracted from 1 cm^3 subsamples following standard procedures (Hendon and Charman, 1997; Booth et al., 2010). At least 100 individual tests were identified following the recommendations of Payne and Mitchell (2009). Taxonomy followed Charman et al. (2000) and Booth (2008). Testate amoebae water table depth (WTD) reconstructions were obtained using the tolerance-downweighted weighted averaging model with inverse deshrinking (WA-Tol inv) from the North American transfer function of Amesbury et al. (2018). Reconstructed WTD values for all sites were then normalised for comparative purposes (Swindles et al., 2015; Amesbury et al., 2016). The variation in reconstructed WTD was assessed using the standard deviation of normalised WTD values (z-scores) within each site.

2.4. Historical climate data

Modelled historical climate data (1901−2010) were obtained for each site using the elevation-dependent ANUSPLIN modelling software (Hutchinson, 2004; McKenney et al., 2011) for comparison with recent reconstructed trends in testate-amoebae inferred peatland WTD. The modelled climate moisture index (CMI; *sensu* Hogg (1997)) represents effective precipitation, which is the principal climatic control of peatland WTDs (Charman et al., 2009). Spatial patterns of average CMI values have been modelled using inverse distance weighting interpolation (IDW power coefficient = 2, resolution = 2 decimal degrees).

3. Results

The majority of testate amoeba assemblage records, with the exceptions of Saco Heath and Petite Bog, are dominated by *Archerella flavum,* an indicator of wet and possibly stable WTD (Charman et al., 2007; Sullivan and Booth, 2011; Amesbury et al., 2013; Lamarre et al., 2013; Turner et al., 2013) (Fig. 3). The assemblage data of Saco Heath and Petite Bog contain high concentrations of the dry indicator species *Hyalosphenia subflava* and the dry-intermediate species *Difflugia pulex* (Charman et al., 2007; Sullivan and Booth, 2011; Amesbury et al., 2013; Lamarre et al., 2013; Turner et al., 2013) (Fig. 3).

The correlation between testate amoeba-inferred WTD reconstructions since 1901 and modelled CMI values for Northern Hemisphere summer months (JJA) over the same time period confirms that moisture availability is the primary driver of WTD values obtained from testate amoeba assemblages at the study sites and that the transfer function is capturing spatial variability in modern moisture content effectively ($R^2 = 0.80$, $P = <0.001$; Fig. 4). These correlations within the modern record justify the application of this transfer function further back in time. Further justification is provided by detrended correspondence analysis (DCA) of the full assemblage data for all sites, which shows that the species ordination along Axis 1 reflects an underlying wetness gradient based on known hydrological preferences of taxa (DCA Axis 1 gradient length = 2.95 and eigenvalue = 0.46; DCA Axis 2 gradient

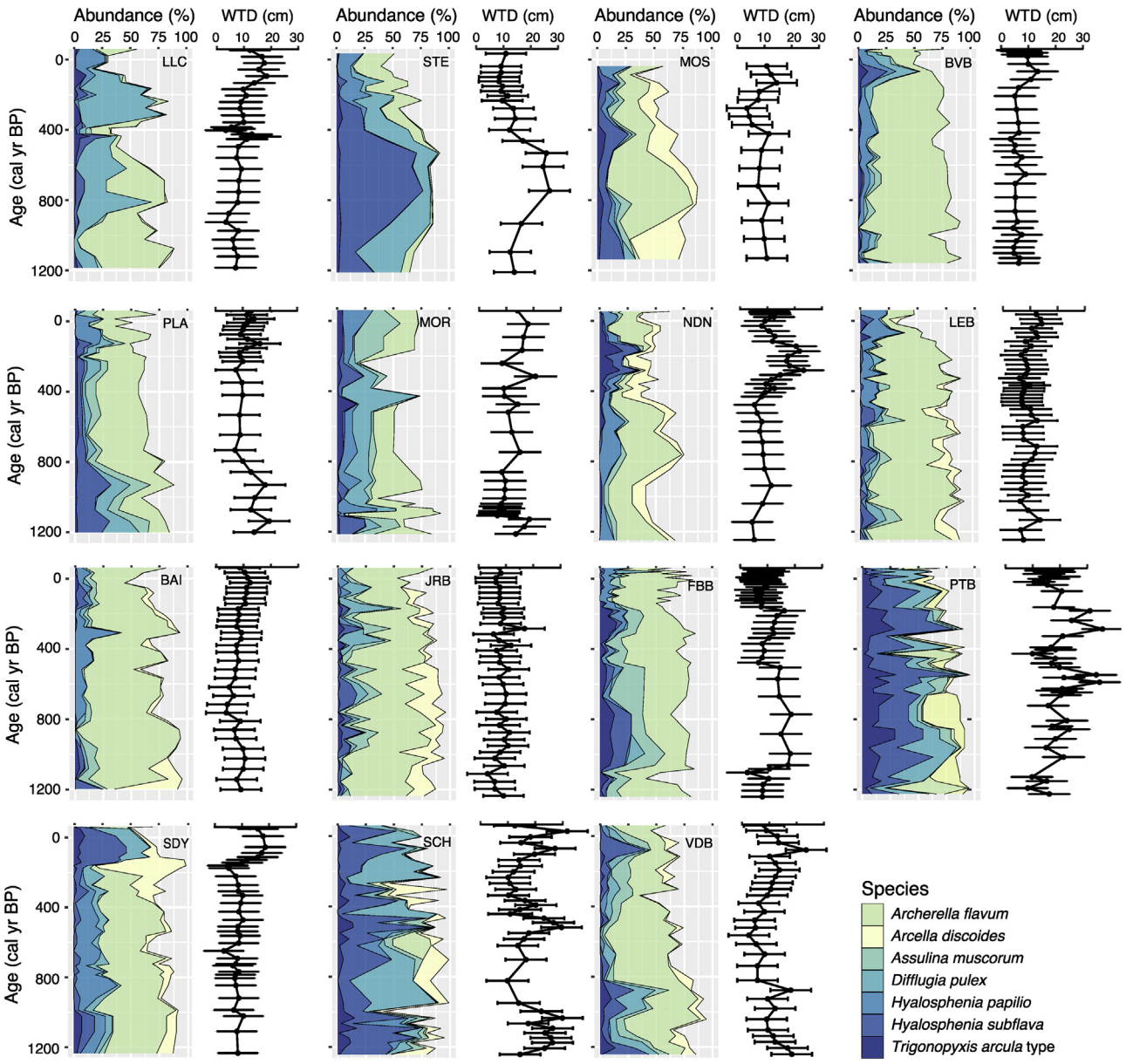

Fig. 3. Summary testate amoebae assemblage data of the seven most abundant taxa across all sites (>3% mean across all sites) (left panel per site) and the corresponding WTD reconstructions (Amesbury et al., 2018) based on the full assemblage data (right panel per site, higher WTD values indicate drier conditions). The seven taxa presented here make up 69 ± 8.5% (1 standard deviation) of the total assemblages at all sites. Sites are ordered from north (top left) to south (bottom right): Lac Le Caron (LLC), Sterne (STE), Mosaik (MOS), Burnt Village Bog (BVB), Plaine (PLA), Morts (MOR), Nordan's Pond Bog (NDN), Lebel (LEB), Baie (BAI), Jeffrey's Bog (JRB), Framboise Bog (FBB), Petite Bog (PTB), Sidney Bog (SDY), Saco Heath (SCH) and Villagedale Bog (VDB).

length = 3.03 and eigenvalue = 0.25; Fig. B1, Table B.1, Supplementary Information). Taxa preferring relatively dry conditions (e.g. *Cryptodifflugia oviformis* type and *Hyalosphenia subflava*) are generally located on the right-hand side of the ordination space and taxa typical of wetter environments (e.g. *Difflugia oviformis* type, *Planocarina carinata* type and *Amphitrema wrightianum*) are located on the left-hand side (Fig. B1, Table B.1, Supplementary Information).

3.1. Testate amoebae-based water table depth reconstructions

Testate amoebae-based WTD reconstructions indicate that on average the hydroclimate of the MCA was wetter relative to pre-MCA conditions at the southern end of the study region in Maine and southern Nova Scotia (Saco Heath, Sidney Bog and Villagedale Bog) and in sites on the north shore of the Gulf of St. Lawrence and the St. Lawrence Estuary (Plaine and Baie) (Fig. 5, Fig. 6A). Conversely, the MCA is associated with a change to a drier hydroclimate in sites in mid-northern Nova Scotia (Framboise Bog, Petite Bog), Newfoundland (Jeffrey's Bog, Nordan's Pond Bog) and James Bay Lowlands (Sterne) (Figs. 5 and 6A). Hydroclimatic conditions are more spatially variable during the LIA compared with the MCA (Fig. 6A, B). Generally, sites in northern Nova Scotia and Newfoundland were relatively wet or becoming wetter during the LIA whilst sites in Maine and many in Québec were relatively dry or becoming drier (Fig. 5). Comparisons of spatial patterns of average LIA and MCA WTDs indicate that wetter MCA conditions were restricted to southern and northern areas of Nova Scotia (Villagedale Bog, Framboise Bog) and James Bay Lowlands (Mosaik, Sterne), whilst sites in Maine (Saco Heath, Sidney Bog) and Newfoundland

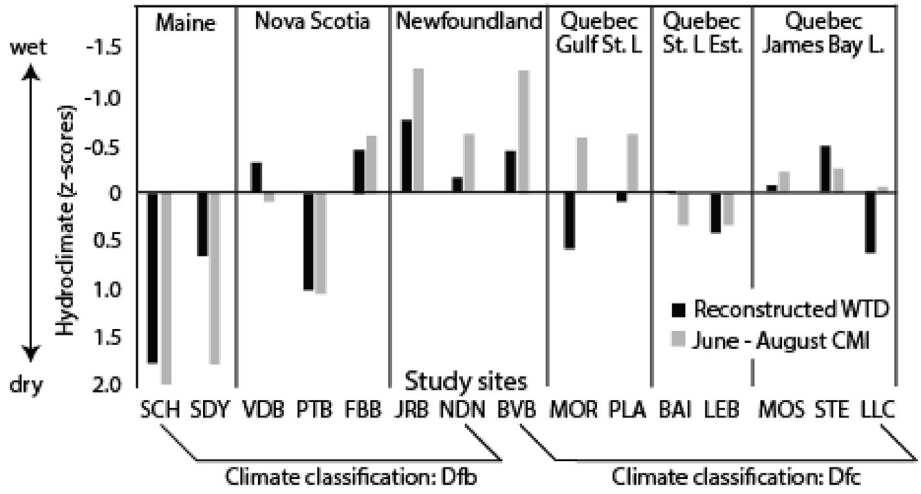

Fig. 4. Average hydroclimatic conditions of each site location from 1901 to 2010 arranged by Köppen-Geiger climate classification zones (snow, fully humid, warm summer (Dfb; left) and snow, fully humid, cold summer and cold winter (Dfc; right) (Kottek et al., 2006)) and geographical regions (left to right): Maine, Nova Scotia, Newfoundland, Gulf of St. Lawrence (Gulf St. L), St. Lawrence Estuary (St. L Est.) and James Bay Lowlands (James Bay L.). Comparison of normalised reconstructed WTD (modelled fossil testate amoebae assemblages using Amesbury et al. (2018) transfer function) and inverse normalised modelled available moisture (CMI) data for average Northern Hemisphere summer conditions (June–August), $R^2 = 0.80$, $P = <0.001$. Sites: Saco Heath (SCH), Sidney Bog (SDY), Villagedale Bog (VDB), Petite Bog (PTB), Framboise Bog (FBB) Jeffrey's Bog (JRB), Nordan's Pond Bog (NDN), Burnt Village Bog (BVB), Morts (MOR), Plaine (PLA), Baie (BAI), Lebel (LEB), Mosaik (MOS), Sterne (STE) and Lac Le Caron (LLC).

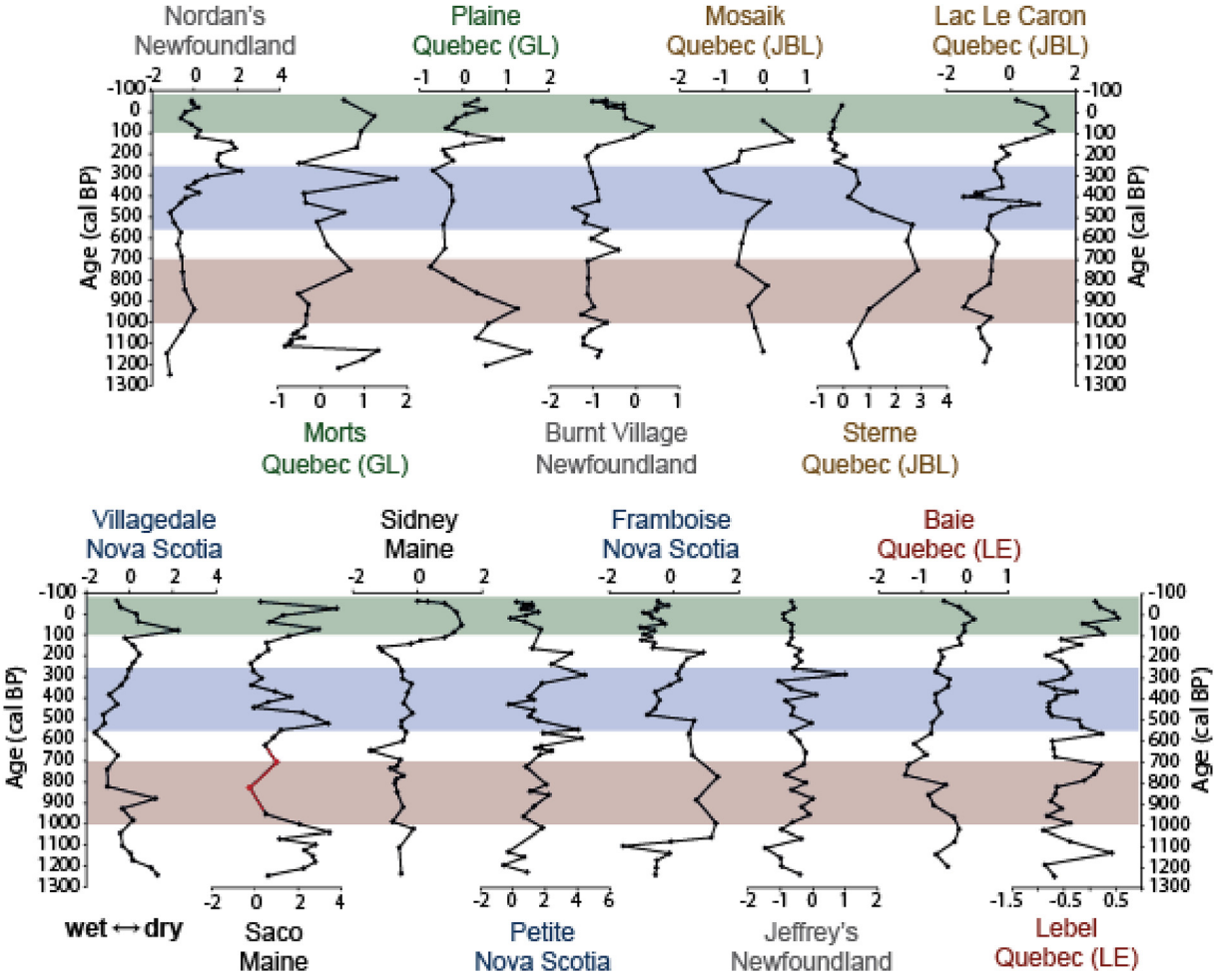

Fig. 5. Normalised testate amoebae inferred WTD reconstructions. Names of sites are coloured by region: Maine in black, Nova Scotia in navy, Newfoundland in grey, Gulf of St. Lawrence, Québec (GL) in green, St. Lawrence Estuary, Québec (LE) in red and James Bay Lowlands, Québec (JBL) in brown. Red highlighted section represents the MCA, blue represents the LIA (as defined by Mann et al., 2009) and green represents the post-LIA period. Lower values represent wetter conditions. Red line in Saco WTD reconstruction represents possible disturbance by fire, as indicated by an increase in the abundance of large charcoal particles (>0.5 mm) identified during macrofossil analysis (Mackay, 2016) and the reduction in accumulation rate during this period (Appendix A.2, Supplementary Information). (For interpretation of the references to colour in this figure legend, the reader is referred to the Web version of this article.)

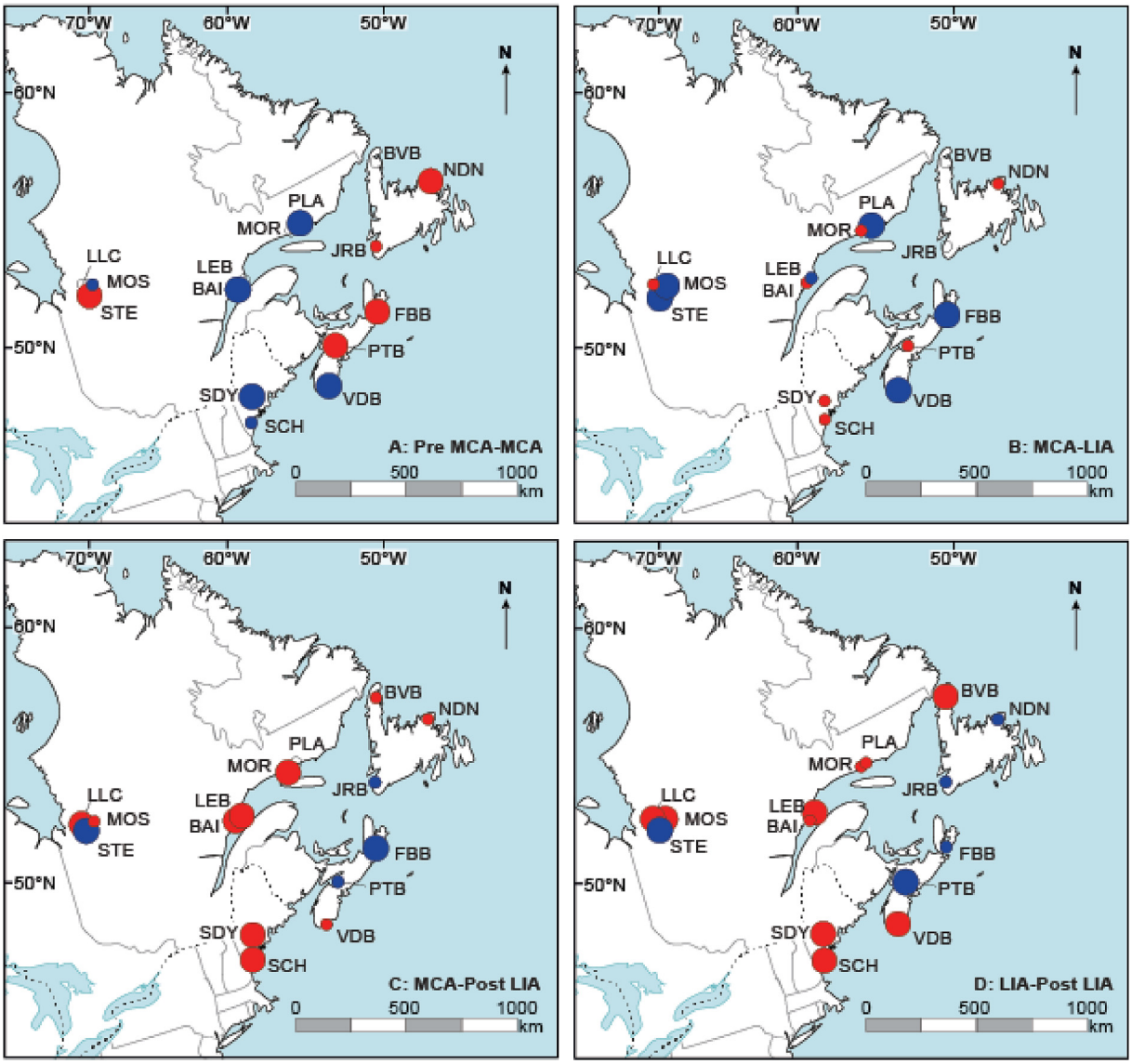

Fig. 6. Spatial patterns of WTD changes between selected time periods: A: Pre-MCA – MCA, B: MCA – LIA, C: MCA – Post LIA, D: LIA – Post LIA. Red circles represent changes to drier conditions and blue circles represent changes to wetter conditions. Larger (smaller) circles indicate changes that are greater (less) than the upper (lower) quartile of standardised WTD from all sites across all time periods. For example in A), red circles are those which are drier in the MCA than they were in the preceding time period (Pre-MCA). Sites with no coloured circles represent small WTD changes that were within 5% of the total WTD range. Sites: Burnt Village Bog (BVB), Nordan's Pond Bog (NDN), Jeffrey's Bog (JRB), Framboise Bog (FBB), Petite Bog (PTB), Villagedale Bog (VDB), Sidney Bog (SDY), Saco Heath (SCH), Lac Le Caron (LLC), Mosaik (MOS), Sterne (STE), Baie (BAI), Lebel (LEB), Morts (MOR), Plaine (PLA). (For interpretation of the references to colour in this figure legend, the reader is referred to the Web version of this article.)

(Nordan's Pond Bog) became drier. Responses differed between neighbouring sites in the St. Lawrence Estuary (Baie, Lebel) and the Gulf of St. Lawrence (Plaine, Morts), with some sites registering drier conditions whilst others registered wetter conditions (Fig. 6B).

During the post-LIA period, sites in mid-northern Nova Scotia and south eastern Newfoundland (Petite Bog, Framboise Bog, Jeffrey's Bog) were wetter than both the MCA and LIA, whilst sites at the latitudinal extremities (in southern Nova Scotia (Villagedale Bog), Maine (Saco Heath, Sidney Bog), northern Newfoundland (Burnt Village Bog)) and some sites in Québec, particularly in the Gulf of Saint Lawrence and St. Lawrence Estuary regions (Lebel, Baie, Morts and Plaine) were drier (Figs. 5, Fig. 6C and D). Average WTD during the post-LIA period (compared with the LIA and MCA) and the MCA (compared with the pre-MCA) differ with opposing directions of average WTD change expressed in all sites in Maine, Nova Scotia and Newfoundland (Fig. 6A,C,D).

The Northern Hemisphere time periods of the MCA (1000-700 cal yr BP) and the LIA (550-250 cal yr BP), as defined by Mann et al. (2009), generally align with coherent WTD changes presented here (Fig. 5). Whilst WTD reconstructions from Framboise Bog suggest that MCA WTD changes begin earlier (*ca.* 1060 cal yr BP) and Jeffrey's Bog and Nordan's Pond Bog WTD trends extend to *ca.* 630 cal yr BP (Fig. 5), both of these dates are within the chronological errors of the ascribed Northern Hemisphere time periods for the MCA (±90 cal yr BP; Appendix A, Supplementary Item). General reconstructed WTD trends during the LIA persist beyond 250 cal yr BP in many sites (Saco Heath, Villagedale Bog, Framboise Bog, Morts, Plaine, Burnt Village Bog and Lac Le Caron). However, WTD in these sites deviate from LIA trends before *ca.* 190 cal yr BP, which is within chronological uncertainty for the Northern Hemisphere time period defined by Mann et al. (2009) and the later regional

date of 100 cal yr BP for the end of the LIA in north-eastern North America (Naulier et al., 2015).

3.1.1. Spatial patterns of variability in reconstructed water table depth

Within site variability in reconstructed WTD was generally higher during the LIA (SD: 0.64) than any other time period (pre-MCA: SD 0.56; MCA: SD 0.57; post-LIA: 0.48) (Fig. 7C and E). Compared with the MCA, these LIA elevated levels of WTD variation appear to be higher in sites in Maine, central Nova Scotia, southern Newfoundland and the James Bay region of Québec (Fig. 7B and C). However, there are no clear trends based on latitude, longitude or climate zone and a student t-test of WTD variability during the MCA and LIA indicates that there is no statistical difference in variability between time periods when all peat records are considered together ($t = 0.9$, $df = 14$, p-value $= -0.4$). The post-LIA period is generally characterised by the lowest within-site variability in reconstructed WTD compared with the pre-MCA, MCA and LIA (Fig. 7D and E). There is a latitudinal pattern of WTD variability in the post-LIA period (Fig. 7D), with highest values concentrated in the southern sites: regionally calculated average standard deviation values demonstrate the pattern, with sites in Nova Scotia and Maine registering two to three times the variability of sites in Newfoundland and Québec. However, once again there are no statistical differences in WTD variability between post-LIA and LIA ($t = 1.5$, $df = 14$, p-value $= 0.2$), post-LIA and MCA ($t = -0.9$, $df = 14$, p-value $= 0.4$) and post-LIA and pre-MCA ($t = -0.3$, $df = 14$, p-value $= 0.8$) when all peat records are considered together.

3.2. Modelled climate in north-eastern North America (1901–2010)

Historical climate data obtained from the ANUSPLIN modelling software (Hutchinson, 2004; McKenney et al., 2011) reveal a south-north decreasing annual temperature trend across the study region (7 to −2.3 °C; $R^2 = 0.93$, $P = <0.001$), which is also reflected in the average growing season length (226 - 146 days; $R^2 = 0.95$, $P = <0.001$) and to a lesser extent in average annual precipitation (743–1264 mm; $R^2 = 0.68$, $P = <0.001$), although there is no significant relationship between latitude and precipitation (Fig. C1, Supplementary Information). The modelled climate moisture index (CMI; *sensu* Hogg (1997)) represents effective precipitation, which is the main climatic control of peatland WTD (Charman et al., 2009). There is no significant relationship between latitude and average modelled CMI during the Northern Hemisphere summer months (JJA) (Fig. 8; Appendix C, Supplementary Information). The CMI indicates that three of the four most southern sites (Saco Heath, Sidney Bog and Petite Bog) have experienced summer moisture deficits (from −1.6 to −0.2 cm) between 1901 and 2010, whilst summer precipitation exceeds evapotranspiration (from 1.1 to 4 cm) at all other sites within this study (Fig. 8; Appendix C, Supplementary Information).

4. Discussion

4.1. MCA hydroclimatic change (1000-700 cal yr BP/950–1250 CE)

North American palaeoenvironmental reconstructions often register drought events during the MCA (e.g. Cook et al., 2010; Ladd et al., 2018; Shuman et al., 2018) that extend from the west coast of the US to the Midwest (Booth et al., 2006, 2012) and the mid-Atlantic states (Cronin et al., 2010; Oswald and Foster, 2011). Some of these events are defined as 'mega-droughts', which are events that persist beyond a decade (Cook et al., 2016). The most prominent dry period during the MCA, reconstructed from peatlands in the western Great Lakes area, occurred *ca.* 1000 cal yr BP, at the start of the MCA (Booth et al., 2006) and this has also been recorded in Mg/Ca ratios from ostracods and oxygen isotopes from benthic foraminifera preserved in marine records obtained from the US east coast in Chesapeake Bay (Cronin et al., 2010). Dry conditions at this time (within chronological errors of *ca.* ±100 years) are evident in WTD records from sites in Maine (Saco Heath), Nova Scotia (Petite Bog, Framboise Bog), Newfoundland (Burnt Village Bog, Nordan's Pond Bog) and Québec (Baie, Lebel, Morts, Plaine, Lac Le Caron) within this study (Fig. 5). However, unlike peatland WTD records in the Great Lakes (Booth et al., 2006), the dry conditions reconstructed here (with the exception of Framboise Bog and Plaine; Fig. 5) are not pronounced and are recorded as smaller shifts relative to WTD lowering during the LIA and post-LIA period. There is, therefore, no clear evidence from multiple adjacent sites at the multi-decadal sampling resolution to support a pronounced 'drought event', centred *ca.* 1000 cal yr BP in terrestrial records from Maine, Nova Scotia, Newfoundland or Québec.

Towards the end of the MCA, two other dry events, centred on *ca.* 800 and 700 cal yr BP, have been recorded in the western Great Lakes area (Booth et al., 2006) and there are prolonged widespread droughts recorded in the Atlantic Palmer Drought Severity Index at *ca.* 850 cal yr BP (Cook et al., 2010, 2011). Some sites within this study do contain dry shifts around these timings: low water tables are reconstructed at 850/800 cal yr BP in some more northerly sites (Petite Bog, Framboise Bog, Jeffrey's Bog, Lebel, Morts, Mosaik, Sterne, Lac Le Caron) and 700 cal yr BP in some more southerly sites (Villagedale Bog, Saco Heath, Jeffrey's Bog, Baie and Lebel) (Fig. 5). However, as was the case with the dry shifts recorded *ca.* 1000 cal yr BP, these dry excursions are not key prominent events within the last millennium. The subtle dry shifts recorded in sites within this study may be the muted manifestations of the drought events centred on more western regions of North America. This therefore suggests that either the climatic drivers of these Medieval drought events have reduced influence in this region of north-eastern North America (owing to North Atlantic oceanic conditions and more abundant moisture sources associated with the majority of study sites) or that other climatic forces were more dominant in this region at this time. Alternatively or additionally, reconstructed water table lowering during the MCA within this study may be related to the warmer MCA temperatures which promoted peat growth and enhanced peat accumulation, thereby creating an autogenically-driven apparent lowering of the water table (e.g. Yu et al., 2003; Swindles et al., 2012).

Whilst drier average hydroclimate conditions during the MCA relative to pre-MCA are evident in WTD reconstructions from sites in central-northern Nova Scotia (Framboise Bog, Petite Bog) and Newfoundland (Jeffrey's Bog, Nordan's Pond Bog), wetter conditions were prevalent at the southern end of the study region in Maine (Saco Heath, Sidney Bog), southern Nova Scotia (Villagedale Bog) and around the Gulf of St. Lawrence (Baie, Plaine) (Figs. 5 and 6A). These results contribute to the growing body of evidence in support of wetter conditions in north-eastern US, particularly in Maine, during times of extreme drought in the western US from palaeoenvironmental records (Shuman et al., 2018). Support for these hydroclimatic spatial patterns is displayed in both modern mid-summer drought records (Cook et al., 2010) and MCA palaeoenvironmental reconstructions. Examples of other reconstructed wetter conditions in the MCA compared with pre-MCA can be found in Maine in pollen records (Gajewski, 1988), lake level reconstructions (Dieffenbacher-Krall and Nurse, 2005) and plant lipid biomarkers (*n*-alkanes) (Nichol and Huang, 2012). Existing studies from Québec also support wetter MCA conditions relative to the LIA

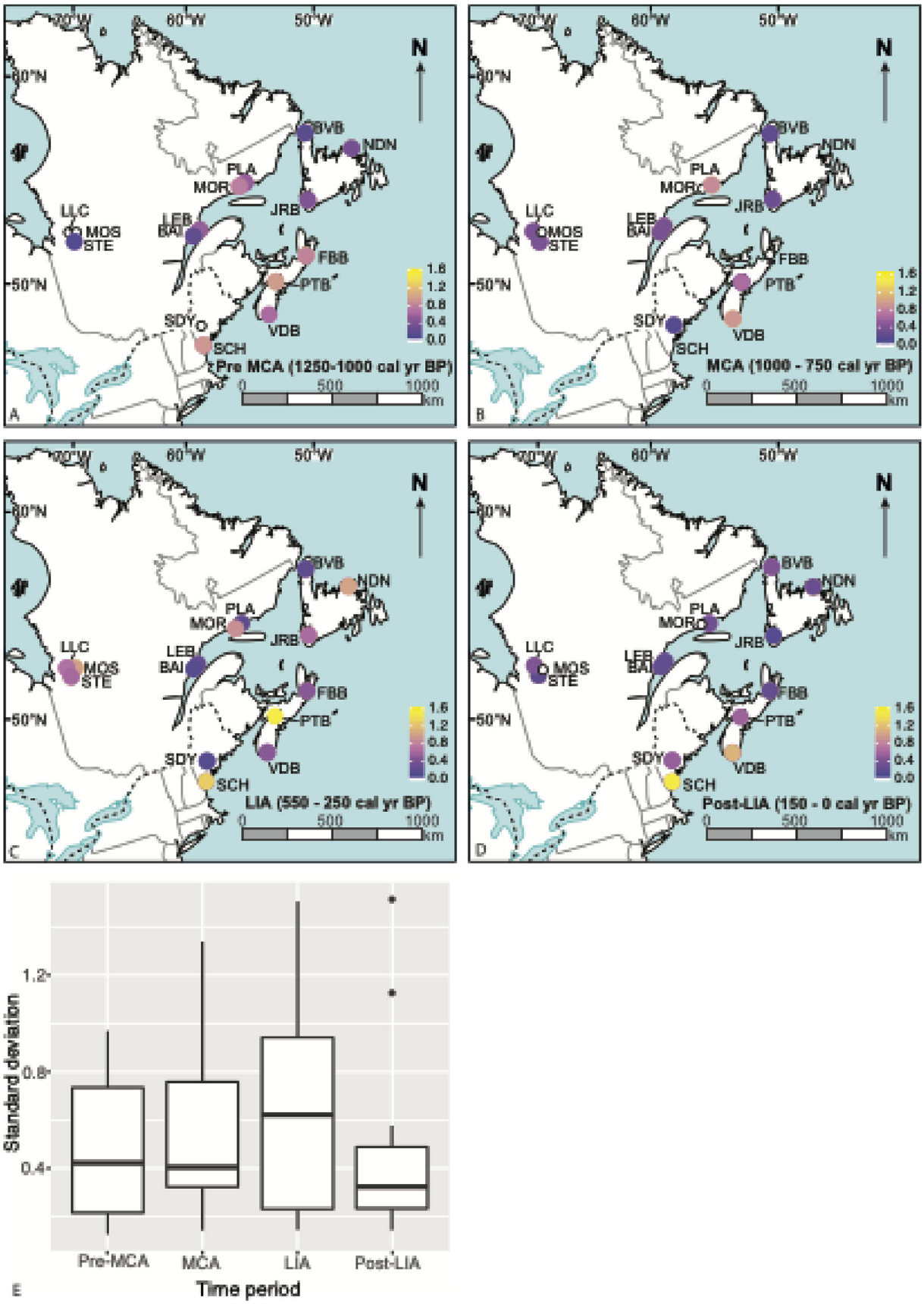

Fig. 7. Comparison of average variation in WTD for A: pre-MCA, B: MCA, C: LIA, D: post-LIA period (for sites with number of samples ≥5, equating to 50-year resolution) and E: boxplot comparison of all sites between different time periods. Variation has been calculated using site-specific standard deviation values of reconstructed WTD for each time period of interest. Variation from low-high is coloured blue-yellow in A-D. Sites: Lac Le Caron (LLC), Mosaik (MOS), Sterne (STE), Baie (BAI), Lebel (LEB), Morts (MOR), Plaine (PLA), Nordan's Pond Bog (NDN), Burnt Village Bog (BVB), Jeffrey's Bog (JRB), Framboise Bog (FBB), Petite Bog (PTB), Villagedale Bog (VDB), Sidney Bog (SDY) and Saco Heath (SCH). (For interpretation of the references to colour in this figure legend, the reader is referred to the Web version of this article.)

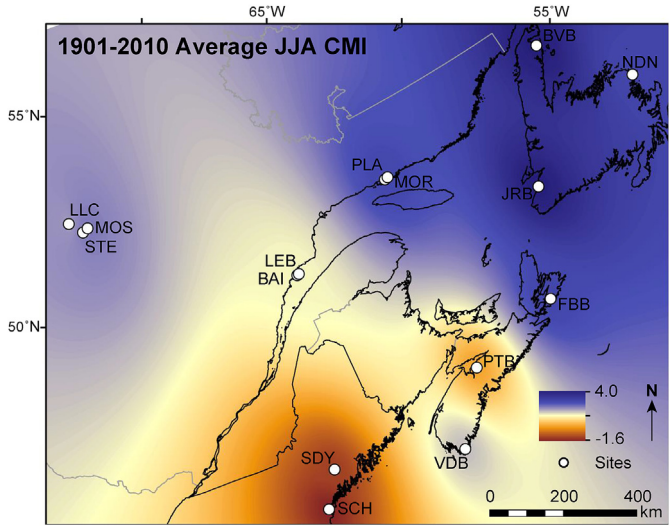

Fig. 8. Spatial patterns of modelled average Climate Moisture Index (CMI) for Northern Hemisphere summer months (June, July, August: JJA) (1901–2010). The CMI represents available moisture (average precipitation - average potential evapotranspiration), from high (blue) to low (yellow). Sites: Lac Le Caron (LLC), Mosaik (MOS), Sterne (STE), Baie (BAI), Lebel (LEB), Morts (MOR), Plaine (PLA), Nordan's Pond Bog (NDN), Burnt Village Bog (BVB), Jeffrey's Bog (JRB), Framboise Bog (FBB), Petite Bog (PTB), Villagedale Bog (VDB), Sidney Bog (SDY) and Saco Heath (SCH). (For interpretation of the references to colour in this figure legend, the reader is referred to the Web version of this article.)

(Paquette and Gajewski 2013; Holmquist et al., 2016), but reveal complex temperature patterns of warmer temperatures proximal to the James Bay Lowlands and cooler temperature in more oceanic regions around the Gulf of St. Lawrence (Viau et al., 2012).

The spatial extent of wet MCA conditions relative to the pre-MCA period in north-eastern North America is restricted to Québec (St. Lawrence Estuary and the Gulf of St. Lawrence), Maine and southern Nova Scotia (Fig. 6A). This north-eastern extent is in agreement with findings from a recent synthesis study that suggested wetter MCA conditions extended to southern Nova Scotia (Shuman et al., 2018). Reconstructed WTD at sites north of Villagedale Bog in Nova Scotia are lower during the MCA relative to pre-MCA WTD (Fig. 6A), as supported by a water table lowering in a peat bog from Prince Edward Island (Peros et al., 2016), which is at a similar latitude. Therefore, a boundary between contrasting hydroclimatic shifts during the MCA in the Atlantic Provinces may lie between the locations of southern Nova Scotia and Prince Edward Island (43.5–46°N).

A notable exception to reconstructed wet MCA conditions in Maine is evident in a previously published record from Sidney Bog, which reported dry conditions throughout the MCA (900–550 cal yr BP) (Clifford and Booth, 2015). This contrasts with the near-surface WTD reconstructed from the same peatland in the present study, which was obtained from a different coring location. These discrepancies in water table reconstructions from the same peatland could either be a result of site-specific conditions at each coring location (e.g wind exposure vs. sheltered areas), non-climate related influences, such as autogenic feedbacks (Swindles et al., 2012) and/or secondary environmental gradients (Juggins, 2013) that could be influencing one or both of these records. Identifying autogenic processes and non-climatic drivers of WTD would require the analyses of more replicate cores obtained from this peatland. However, confidence in the reconstruction obtained from this study is provided by the aforementioned proximal records, which support regionally wet conditions during the MCA in the south of study area.

4.2. LIA hydroclimatic change (550–250 cal yr BP/1400–1700 CE)

The WTD spatial trends reconstructed for the beginning of the LIA in this study indicate a north east/south west split in hydrological conditions of opposing conditions compared with MCA WTDs: sites in northern Nova Scotia and Newfoundland were wet or becoming wetter whilst sites in Maine and many in Québec were dry or becoming drier (Fig. 5). Such dry conditions at the start of the LIA have also been reported from a synthesis of North American drought data (Cook et al., 2009).

Average LIA hydroclimate conditions show a complex spatial pattern with wet conditions restricted to sites of James Bay Lowlands and southern and northern Nova Scotia (Figs. 5 and 6B). This spatial pattern of hydroclimate change is supported by some other published proximal records: WTD reconstructions obtained from a peatland in Prince Edward Island reported wet conditions during the LIA (Peros et al., 2016) and drought events are reported between 500 and 600 cal yr BP from other peatland WTD reconstructions in Maine (Clifford and Booth, 2013; Clifford and Booth, 2015). Pollen-based temperature reconstructions also reveal similar spatial trends with cooler LIA temperatures in the region surrounding the James Bay Lowlands and Nova Scotia (Viau et al., 2012). However, not all existing paleoenvironmental records support these average LIA climatic spatial patterns: higher lake levels were reconstructed during the LIA elsewhere in Maine (Dieffenbacher-Krall and Nurse, 2005), as reflected in a review of north-eastern US Late Holocene climate, which identified elevated moisture levels and/or reduced drought events throughout the LIA from 550 cal yr BP (Marlon et al., 2017). Furthermore, dry conditions are recorded at *ca.* 600 cal yr BP in the south-west of Québec based on pollen records obtained from lake sediments (Paquette and Gajewski, 2013; Lafontaine–Boyer and Gajewski, 2014) and more frequent fires during the LIA until 1850 CE in western Québec indicate the dominance of dry Arctic air mass during this time (Bergeron et al., 2004).

The complex and varying spatial patterns in LIA WTDs that have emerged across the study region may be attributed to hydroclimatic variability and/or site-specific sensitivities to hydroclimate change. More variable climatic conditions during the LIA compared with the MCA have been reported from elsewhere in this region (Lafontaine-Boyer and Gajewski, 2014; Holmquist et al., 2016). The peatland WTD variability between the LIA and MCA was not statistically different when all sites in this study were considered together. However, elevated within-peatland multi-decadal hydroclimate variation during the LIA was identified in reconstructions from James Bay Lowlands and sites in Maine and Nova Scotia (Fig. 7). Site-specific sensitivities to hydroclimate change during the LIA may relate to local permafrost aggradation and limited snow accumulation, both of which would create relatively dry, highly localised conditions. For example, the hydrological regimes of the exposed northern peatlands in Québec and Newfoundland may have been affected by persistent frozen layers at times during the LIA, as proposed by Van Bellen et al. (2011) to explain reconstructed peatland palaeohydrological trends in James Bay Lowlands. In addition, treeless coastal peatlands, such as those located along the Gulf of St. Lawrence, are highly exposed to winds which can limit snow accumulation during winter, allowing for the build-up of frozen peat layers and removing the additional snow water supply at the start of the growing season (Magnan and Garneau, 2014).

Many of the sites analysed in this study contain pronounced wet and dry shifts during the LIA (Fig. 5) but there is little consistency in the pattern of these events between sites since they vary in timing, duration and extent. The exception to this is the change towards

drier conditions in all peatlands centred *ca*. 400 cal yr BP (1500 CE) (Fig. 5), a time of cold temperatures and permafrost development in Québec (Arlen-Pouliot and Bhiry, 2005; Fillion et al., 2014). Whilst this widespread dry-shift may reflect an apparent drying in northern peatlands affected by frost, the timing of this dry-shift may also correspond to a mega drought reported in the 16th century across North America (Ladd et al., 2018), thus extending its known eastern extent.

Tree-ring based temperature reconstructions from the Québec-Labrador Peninsula show that regional terrestrial LIA cooling began in 1450 CE (Naulier et al., 2015), with the coolest phase of the LIA detected following the Tambora eruption in 1815 CE until the middle of the 19th century (Gennaretti et al., 2014). This LIA temperature minimum in the Québec-Labrador Peninsula was therefore a century later than the coolest LIA phase detected when the Northern Hemisphere is considered as a whole (1700 CE, Mann et al., 2009). Similarly, the 19th century was highlighted as a particularly cold period at the St. Lawrence River at Québec City based on historical records of ice bridge formation (Houle et al., 2007). The site-specific LIA trends of reconstructed WTD from this study do extend beyond 1700 CE (Fig. 5) and are comparable with 19th century regional dates (Naulier et al., 2015). However, chronological uncertainties for the majority of study sites overlap both time periods and therefore preclude refinement of LIA timings within this study.

4.3. Post-LIA (1850 CE-present day) hydroclimatic change

Reconstructed temperatures from the Gulf of St. Lawrence indicate that 20th century warming was greater than any experienced during the last millennium (Thibodeau et al., 2010) and records of precipitation across the study region show increases that are projected to continue because of increases in the concentration of atmospheric water vapour (Kunkel et al., 2013). All sites within this study, with the exception of Jeffrey's Bog in southern Newfoundland, exhibit pronounced WTD changes during the post-LIA period at the multi-decadal sampling resolution (Fig. 5) and a complex spatial pattern of hydroclimate change is evident across the study region: sites in the middle of the study region (mid-northern Nova Scotia and southern and eastern Newfoundland) are reconstructed as wetter than preceding periods, whilst sites at the latitudinal extremities (Maine, southern Nova Scotia and northern Newfoundland) and some sites in Québec are drier (Fig. 6C and D). These hydroclimatic spatial patterns are consistent across comparisons of both the MCA to post-LIA period and the LIA to post-LIA period (Fig. 6C and D).

The unstable hydroclimate conditions in Maine and southern Nova Scotia in the post-LIA period may be caused by their proximity to sub-tropical storm tracks, which bring intense rainfall events to this region and could enhance variability in WTD. Whilst several studies have demonstrated that summertime extratropical cyclones have been decreasing in frequency since the 1980's (e.g. Chang et al., 2016; Colle et al., 2013), the intensity of these storms and the amount of precipitation that they deliver have increased because warmer temperatures increase the capacity of the atmosphere to hold water vapour (Pfahl et al., 2015; Colle et al., 2013). Under projected future climate warming, hurricane intensity in the North Atlantic basin is projected to further increase over the late 21st century, increasing precipitation rates and the number and occurrence days of category 4 and 5 storms (Knutson et al., 2015; Ting et al., 2019). Rapid increases in hurricane intensity are facilitated by reduced vertical wind shear along the U.S East Coast, which acts as a protective barrier to hurricanes, and greater sea surface temperature warming in this region (Ting et al., 2019).

4.4. Spatial expression of MCA and LIA hydrological change: implications for climate drivers

Reconstructed expressions of climate drivers during the MCA support a combined ocean-atmosphere climatic forcing mechanism: the Atlantic Multidecadal Oscillation (AMO) was in a persistent positive warm phase (Mann et al., 2009; Steiger et al., 2019) and the North Atlantic Oscillation (NAO) was in a positive phase (e.g. D'Arrigo et al., 2006; Trouet et al., 2009; Cronin et al., 2010). Whilst recent analysis of observational data and climate model simulations have demonstrated that the AMO signal is not distinguishable from climatic noise background (Mann et al., 2020), the associated climatic manifestations in eastern North America include a strengthening of the Polar Vortex thus generating a more zonal Polar Jet Stream and a northward storm track shift across the eastern Atlantic (Ineson et al., 2011; Martin-Puertas et al., 2012) (Fig. 9). The resultant increase in winter storm precipitation during the MCA in north-eastern North America would be accompanied by increases in summer-autumn precipitation arising from increases in the frequency and greater northwards extension of tropical cyclones (Mann et al., 2009).

Increases in reconstructed moisture availability during the MCA were restricted to the sites in the south of the study region in Maine, southern Nova Scotia and sites in Québec proximal to the Gulf of St. Lawrence and the St. Lawrence Estuary, whereas sites in northern Nova Scotia, Newfoundland and Quebec's James Bay Lowlands were drier (Fig. 6A). Warm MCA temperatures would promote peatland productivity rates, particularly in northern sites with cooler average temperatures, and therefore contribute an autogenically-driven lowering of the WTD. However, the spatial patterns of reconstructed hydroclimatic trends most likely support a narrowing of the Westerly Wind belt, with a latitudinal limit in southern Nova Scotia, and elevated hurricane activity between southern Nova Scotia and southwestern regions of the Gulf of St. Lawrence and St. Lawrence Estuary (Fig. 9).

The lack of evidence for pronounced Medieval drought events in north-eastern North America (Section 4.1) may be a result of the sampling resolution within this study (*ca*. 40 years), since such events may not be captured in the WTD records or may only be registered as a hydrological excursion in one sample. However, the results from this study are in support of the growing body of evidence that there was a Pacific-based Medieval mega-drought driver (e.g. Coats et al., 2016), as first postulated by Booth et al. (2006) based on peatland records of hydroclimatic change in the western Great Lakes region. Steiger et al. (2019) have recently refined the theory behind climatic drivers of medieval drought through analysis of modelled hydroclimate conditions from the Palaeo Hydrodynamic Data Assimilation product (Steiger et al., 2018).

Spatial patterns of WTD changes within north-eastern North America at the start of the LIA were opposite to those expressed during the MCA: sites in Maine and many in Québec were dry or becoming drier whilst sites in northern Nova Scotia and Newfoundland were wet or becoming wetter (Fig. 5). These trends can therefore be explained by the switch to the negative phase of the NAO at the beginning of the LIA (e.g. Cronin et al., 2010), which would have contributed towards a reduction in the strength of the Polar Vortex and thus generated a meridional flow of the Polar Jet Stream (Ineson et al., 2011; Martin-Puertas et al., 2012) and long-term movement of storm tracks (Bakke et al., 2008) (Fig. 9).

A recent review of late Holocene North Atlantic Ocean circulation by Moffa-Sánchez et al. (2019) highlights that MCA-LIA changes are difficult to reconcile because of differences in palaeoenvironmental reconstructions. For example, some studies have supported an AMOC slow down during the LIA (Lund et al., 2006),

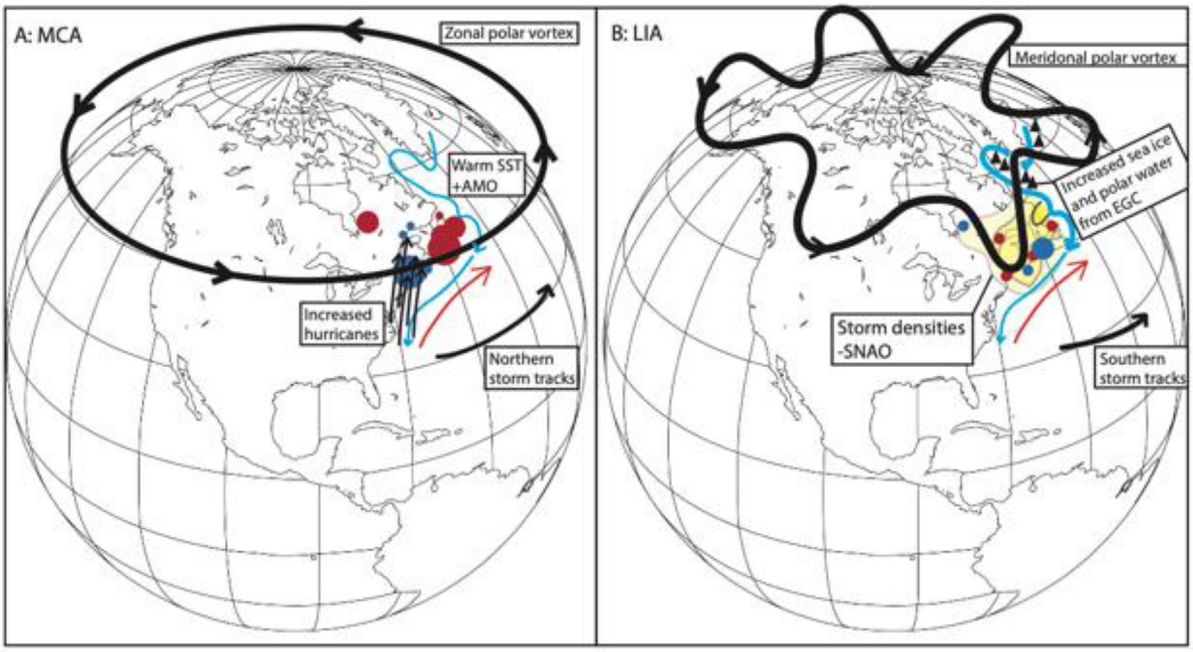

Fig. 9. Synoptic climate map highlighting main climatic influences on MCA and LIA hydroclimate in north-eastern North America. SST = sea surface temperatures, AMO = Atlantic Multidecadal Oscillation, SNAO = summer North Atlantic Oscillation (storm densities represented by yellow shading with darker (lighter) yellow representing greater (fewer) storm densities), EGC = East Greenland Current. Blue and red circles respectively represent wet and dry reconstructed WTD at the study sites. Light blue arrows represents cold Labrador Current and red arrow represents warm Gulf Stream. (For interpretation of the references to colour in this figure legend, the reader is referred to the Web version of this article.)

whilst others have inferred an AMOC strengthening (Rahmstorf et al., 2015; Thornalley et al., 2018). Commonalities between several studies do, however, support a cooling and increased drift ice export from north-east Greenland to the subpolar North Atlantic likely within the East Greenland Current (EGC) during the LIA, increasing the amount of polar waters reaching the Labrador-Baffin Bay region relative to Atlantic waters (Moffa-Sánchez et al., 2019). This would therefore reduce sea surface temperatures in areas proximal to the northern oceanic sites within this study (Nordan's Pond Bog, Burnt Village Bog).

The spatial pattern of hydroclimate conditions across the study region is more complex when average LIA hydroclimatic conditions are considered, with more spatially variable average patterns of WTD change emerging compared with both the MCA and initial LIA conditions (Figs. 5 and 6B). The spatial patterns of reconstructed LIA WTD resemble patterns of Atlantic storm density tracks associated with a negative Summer North Atlantic Oscillation (SNAO) (Dong et al., 2013, Fig. 9). The SNAO, which is driven by the AMO (Sutton and Dong, 2012; Dong et al., 2013), has been reconstructed to have been in a persistent negative phase during the latter half of the LIA (Linderholm and Folland, 2017) and may therefore have played a role in shaping average LIA hydroclimatic conditions across the study region.

4.5. Last millennium environmental change as context for current and projected future conditions

The MCA is often referred to as a partial analogue for current and future climate change since it was associated with warmer conditions. However, reconstructed differences in interannual hydroclimate variability between the MCA and the LIA in the American southwest led Loisel et al. (2017) to conclude that the MCA may be a misleading analogue for future climate since interannual LIA hydroclimate conditions were more variable and more similar to 21st century projections than MCA hydroclimate. The multi-decadal peatland WTD reconstructions from north-eastern North America in this study also reveal more stable site-specific WTD reconstructions during the MCA than the LIA. However, these differences in variability are not statistically different when all study sites are considered together, indicating that the variability recorded across the study region is likely related to peatland-specific conditions rather than regional-scale hydroclimate variability. The post-LIA spatial patterns of reconstructed peatland WTD in north-eastern North America from this study are more similar to the LIA than the MCA, as many sites in northern Nova Scotia and southern Newfoundland that became drier during the MCA became wetter during the LIA and post-LIA period (Fig. 6A,C,D). However, the 'warm LIA' scenario, suggested as an analogue for future hydroclimate variability by Loisel et al. (2017), is likely not appropriate for peatlands of north-eastern North America since it cannot account for important regional mesoclimatic LIA influences, such as permafrost aggradation, which impact peat hydrology and accumulation dynamics in this region.

5. Conclusions

Analysis of the testate amoebae-based water table reconstructions developed from peatlands in north-eastern North America has identified complex hydroclimatic spatial trends that varied over the last millennium. Climatic changes associated with the Medieval Climate Anomaly (MCA) and the Little Ice Age (LIA) have been detected in these peat records; however, such changes are not uniform across the region. Southern peatlands were relatively wet during the MCA, whilst northern and more continental sites were relatively dry. This spatial trend in MCA hydroclimate supports findings from other recent regional palaeoenvironmental reconstructions such as Ladd et al. (2018) and Shuman et al. (2018), and helps to constrain the northern geographical limit of these wet MCA conditions to southern Nova Scotia. West and Mid-West American MCA drought events do register as dry shifts in these

north-eastern records; however, they are not prominent hydroclimatic features. There is therefore no evidence that the Medieval droughts extended across the Atlantic seaboard of north-eastern North America, based on the multi-decadal resolution of WTD reconstructions from this study. This finding is consistent with the hypothesis that MCA mega-droughts were primarily forced from Pacific climate drivers (e.g. Steiger et al., 2019). Future research that develops palaeoclimate records from currently under-represented areas in north-eastern North America, including New Brunswick and Maine, would help to further characterise late Holocene regional climate variability and test the absence of Medieval droughts in this region.

LIA hydroclimate change in north-eastern North America was often spatially and temporally variable rather than displaying clear WTD directional shifts or latitudinal trends. These variable regional palaeoenvironmental reconstructions support conclusions from synthesis papers, which demonstrate that some dry periods in the LIA were comparable with those reconstructed during the MCA (Ladd et al., 2018; Mann et al., 2009), despite manifesting from different climate forcings or peat hydrological influences such as LIA drying due to local permafrost aggradation. The spatial patterns of peatland WTD reconstructed in this study indicate that the MCA and LIA expressions of climate were likely influenced by complex interactions of external and internal climate drivers and feedbacks that contributed towards a more zonal Polar Jet Stream and increased hurricane activity during the MCA and a meridional Polar Jet Stream flow, combined with Atlantic storm precipitation patterns and extensions of cold polar waters during the LIA. The spatial and temporal diversity of peatland responses to hydrological change reconstructed in this study highlights the complex balance between regional hydroclimate variability and internal peatland dynamics that occurred in north-eastern North America over the last millennium.

Credit author statement

Helen Mackay: Conceptualization, Methodology, Investigation, Formal analysis, Writing – original draft. Matthew J. Amesbury: Conceptualization, Methodology, Investigation, Writing – review & editing. Pete G. Langdon: Conceptualization, Supervision, Writing – review & editing. Dan J. Charman: Conceptualization, Supervision, Writing – review & editing. Gabriel Magnan: Conceptualization, Investigation, Writing – review & editing. Simon van Bellen: Conceptualization, Investigation, Writing – review & editing. Michelle Garneau: Conceptualization, Writing – review & editing. Rupert Bainbridge: Visualization. Paul D. M. Hughes: Conceptualization, Supervision, Writing – review & editing

Funding sources

Funding: This work was supported by the UK Natural Environment Research Council (PRECIP project grants NE/G019851/1, NE/G020272/1, NE/GO19673/1 and NE/GO 2006X/1 and MILLIPEAT project grant NE/1,012,915/1). A Quaternary Research Association New Research Workers award granted to H. Mackay and this work was supported by the NERC Radiocarbon Facility NRCF010001 (allocation numbers 1744.1013 and 1789.0414).

Declaration of competing interest

The authors declare that they have no known competing financial interests or personal relationships that could have appeared to influence the work reported in this paper.

Acknowledgements

Thanks to Gunnar Mallon and Tim Daley for fieldwork assistance and for contributing to the NERC-PRECIP project alongside Alayne Street-Perrott and Neil Loader.

Appendix A

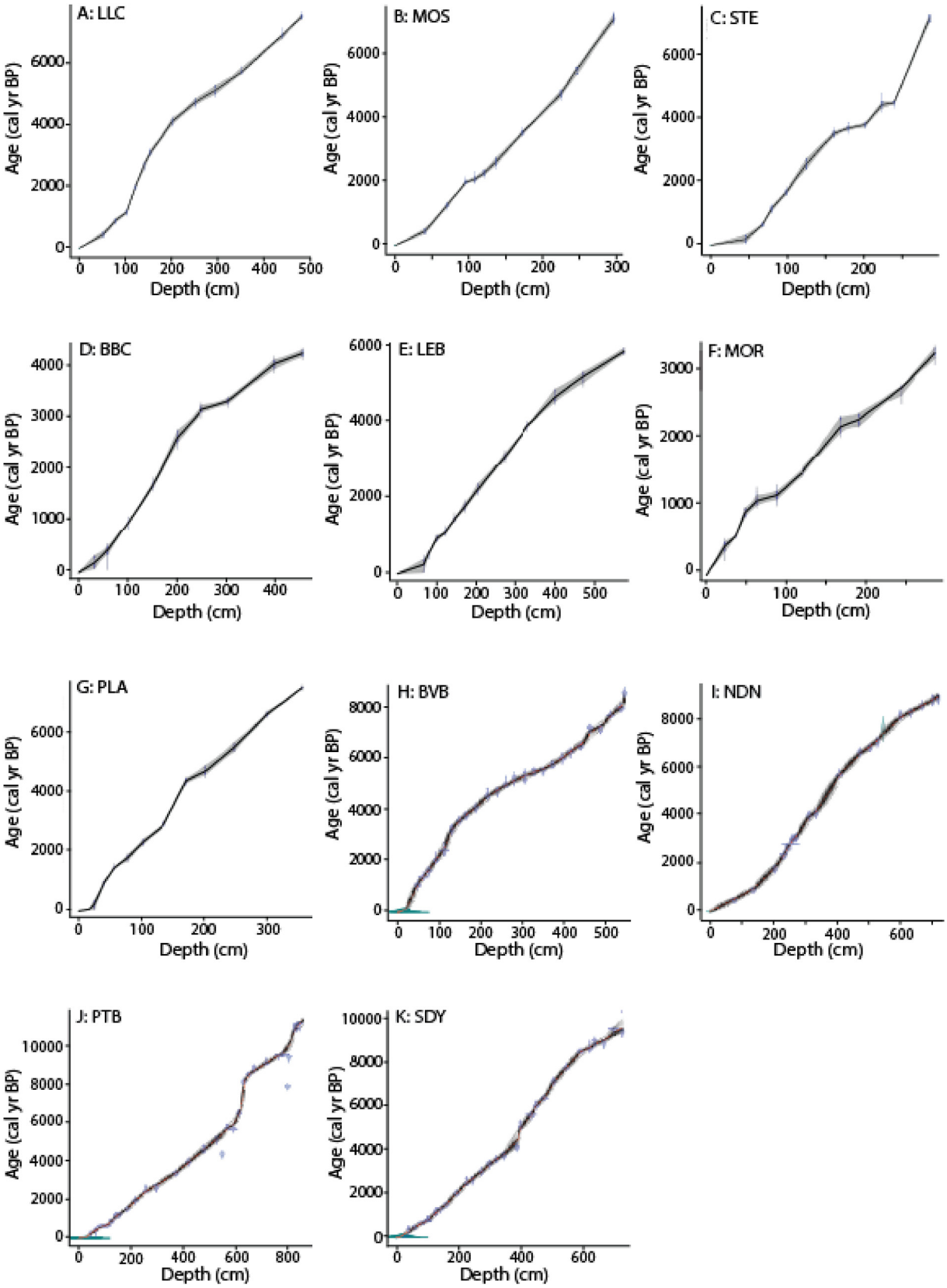

Fig. A1. Published age-depth models for cores A: Lac Le Caron (LLC), B: Mosaik (MOS), C: Sterne (STE), D: Baie (BBC), E: Lebel (LEB), F: Morts (MOR), G: Plaine (PLA), H: Burnt Village Bog (BVB), I: Nordan's Pond Bog (NDN), J: Petite Bog (PTB), K: Sidney Bog (SDY). For full chronological information see original publications: A-C (van Bellen et al., 2011), D-G (Magnan and Garneau, 2014), H–K (Charman et al., 2015).

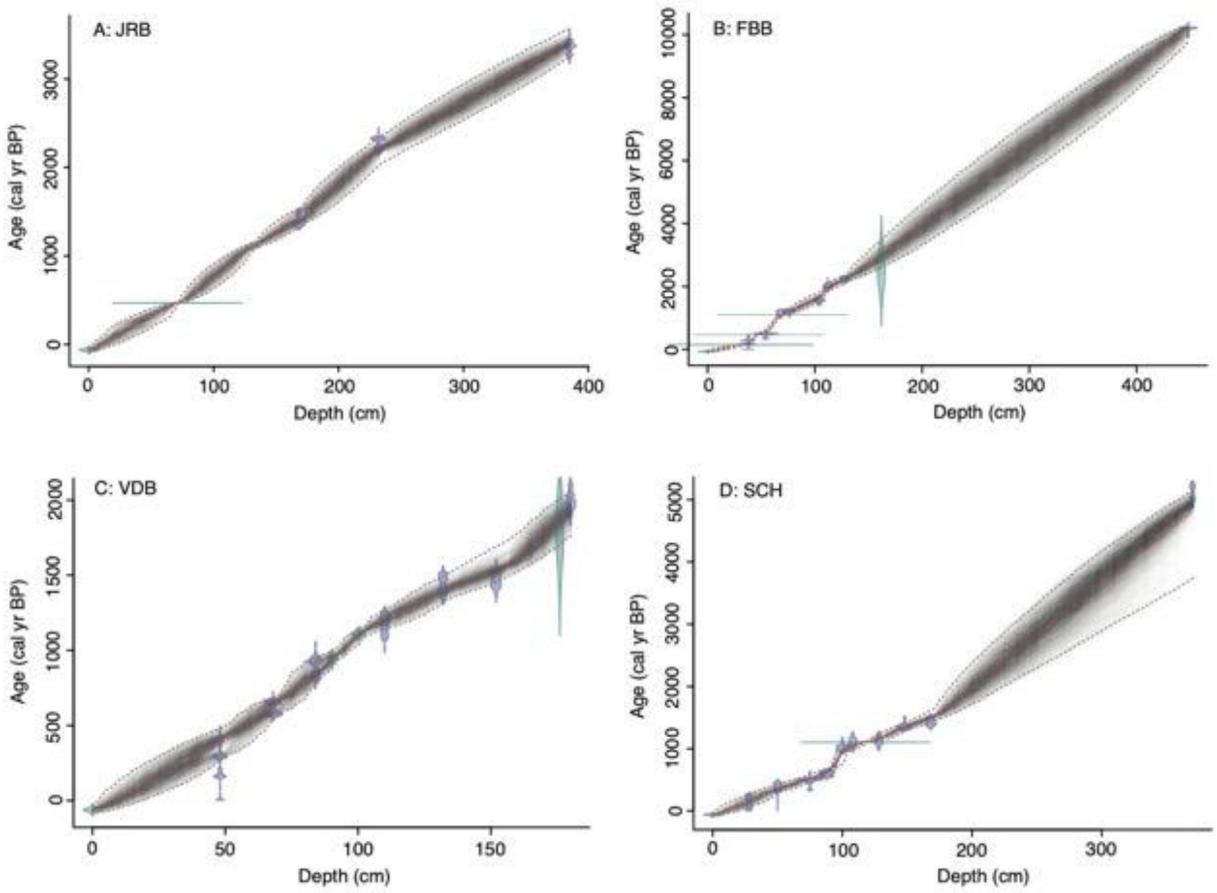

Fig. A2. Updated age-depth models for A: Jeffrey's Bog (JRB), B: Framboise Bog (FBB), C: Villagedale Bog (VDB) and D: Saco Heath (SCH) based on radiocarbon measurements and identified cryptotephras from Mackay et al. (2016). Markov Chain Monte Carlo iterations have been completed in Bacon. The darker areas represent the most likely age ranges.

Appendix B

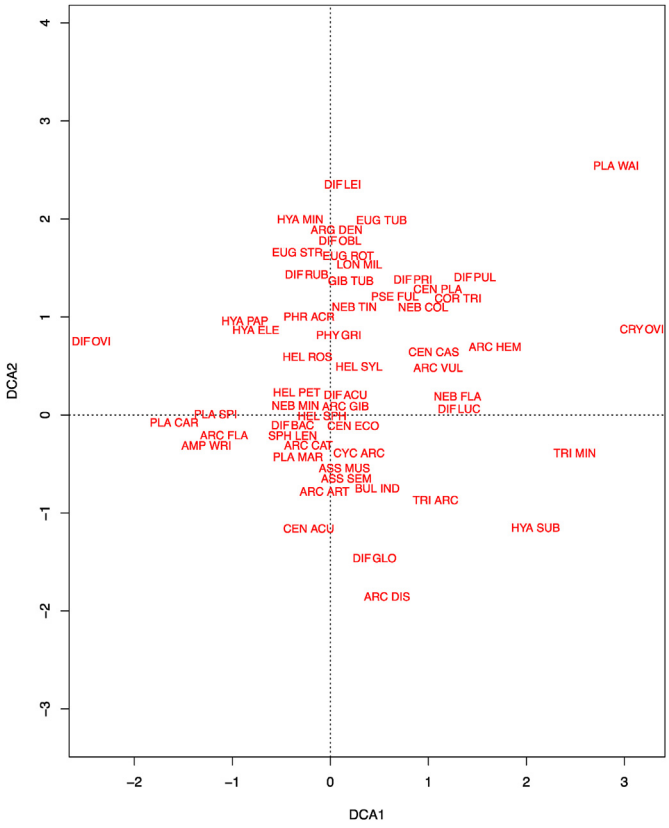

Fig. B1. Detrended Correspondence Analysis (DCA) bioplot of the full testate amoebae assemblage dataset for all sites showing taxa positions (slightly adjusted for readability, ensuring relative between-taxa positions remain the same). DCA Axis 1 gradient length = 2.95 and eigenvalue = 0.46; DCA Axis 2 gradient length = 3.03 and eigenvalue = 0.25. Species ordination along Axis 1 reflects an underlying wetness gradient based on known hydrological taxa.

Table B.1
Testate amoeba taxonomy applied in this study

Abbreviation	Full name
AMP WRI	*Amphitrema wrightianum* type
ARC ART	*Arcella artocrea*
ARC CAT	*Arcella catinus* type
ARC DIS	*Arcella discoides* type
ARC GIB	*Arcella gibbosa* type
ARC HEM	*Arcella hemispherica* type
ARC VUL	*Arcella vulgaris* type
ARC FLA	*Archerella flavum*
ARG DEN	*Argynnia dentistoma* type
ASS MUS	*Assulina muscorum*
ASS SEM	*Assulina seminulum* type
BUL IND	*Bullinularia indica*
CEN ACU	*Centropyxis aculeata* type
CEN CAS	*Centropyxis cassis* type
CEN PLA	*Centropyxis platystoma* type
CEN ECO	*Centropyxis ecornis* type
COR TRI	*Corythion − Trinema* type
CRY OVI	*Cryptodifflugia oviformis* type
CYC ARC	*Cyclopyxis arcelloides* type
DIF ACU	*Difflugia acuminata* type
DIF BAC	*Difflugia bacillifera* type
DIF GLO	*Difflugia globulosa* type
DIF LEI	*Difflugia leidyi*
DIF LUC	*Difflugia lucida* type
DIF OBL	*Difflugia oblonga* type
DIF OVI	*Difflugia oviformis* type
DIF PRI	*Difflugia pristis* type
DIF PUL	*Difflugia pulex* type
DIF RUB	*Difflugia rubescens* type
EUG ROT	*Euglypha rotunda* type
EUG STR	*Euglypha strigosa* type
EUG TUB	*Euglypha tuberculata* type
GIB TUB	*Gibbocarina (Nebela) tubulosa* type
HEL ROS	*Heleopera rosea*
HEL PET	*Heleopera petricola*
HEL SPH	*Heleopera sphagni*
HEL SYL	*Heleopera sylvatica*
HYA ELE	*Hyalosphenia elegans*
HYA MIN	*Hyalosphenia minuta*
HYA PAP	*Hyalosphenia papilio*
HYA SUB	*Hyalosphenia subflava*
LON MIL	*Longinebela (Nebela) militaris* type
NEB COL	*Nebela collaris* type
NEB FLA	*Nebela flabellulum*
NEB MIN	*Nebela minor*
NEB TIN	*Nebela tincta* type
PHR ACR	*Phryganella acropodia* type
PHY GRI	*Physochila griseola* type
PLA SPI	*Placocista spinosa* type
PLA CAR	*Planocarina (Nebela) carinata* type
PLA MAR	*Planocarina (Nebela) marginata* type
PLA WAI	*Padaungiella (Nebela) wailesi*
PSE FUL	*Pseudodifflugia fulva* type
SPH LEN	*Sphenoderia lenta*
TRI ARC	*Trigonopyxis arcula* type
TRI MIN	*Trigonopyxis minuta* type

Appendix C

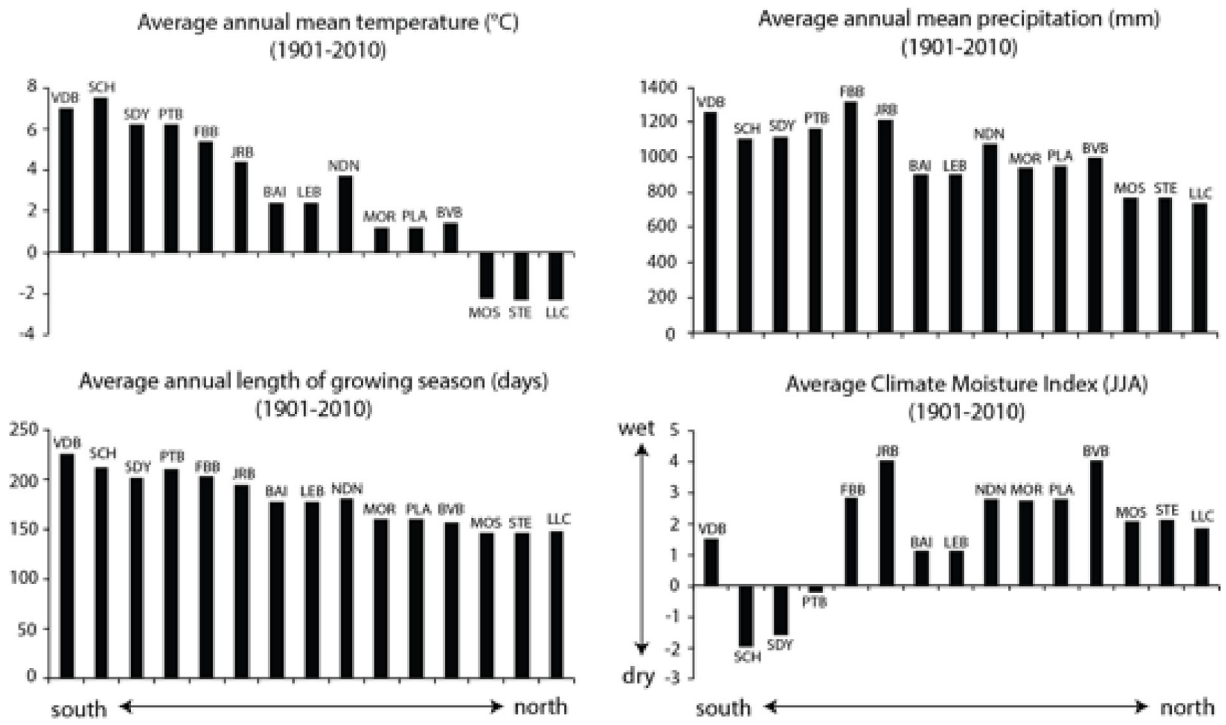

Fig. C1. Average modelled climate data for each site location (ordered from south (left) to north (right)) from 1901 to 2010, extracted from the elevation-dependent ANUSPLIN modelling software (Hutchinson, 2004; McKenney et al., 2011). The Climate Moisture Index represents available moisture (ratio of average precipitation to average potential evapotranspiration) across the Northern Hemisphere summer months (June, July and August). Sites: Villagedale Bog (VDB), Saco Heath (SCH), Sidney Bog (SDY), Petite Bog (PTB), Framboise Bog (FBB) Jeffrey's Bog (JRB), Baie (BAI), Lebel (LEB), Nordan's Pond Bog (NDN), Morts (MOR), Plaine (PLA), Burnt Village Bog (BVB), Mosaik (MOS), Sterne (STE) and Lac Le Caron (LLC).

References

Amesbury, M.J., Mallon, G., Charman, D.J., Hughes, P.D.M., Booth, R.K., Daley, T.J., Garneau, M., 2013. Statistical testing of a new testate amoeba-based transfer function for water-table depth reconstruction on ombrotrophic peatlands in north-eastern Canada and Maine, United States. J. Quat. Sci. 28, 27–39.

Amesbury, M.J., Swindles, G.T., Bobrov, A., Charman, D.J., Holden, J., Lamentowicz, M., Mallon, G., Mazei, Y., Mitchell, E.A.D., Payne, R.J., Roland, T.P., Turner, T.E., Warner, B.G., 2016. Development of a new pan-European testate amoeba transfer function for reconstructing peatland palaeohydrology. Quat. Sci. Rev. 152, 132–151.

Amesbury, M.J., Booth, R.K., Roland, T.P., Bunbury, J., Clifford, M.J., Charman, D.J., Elliot, S., Finkelstein, S., Garneau, M., Hughes, P.D.M., Lamarre, A., Loisel, J., Mackay, J., Magnan, G., Markel, E.R., Mitchell, E.A.D., Payne, R.J., Pelletire, N., Roe, H., Sullivan, M.E., Swindles, G.T., Talbot, J., Van Bellen, S., Warner, B.G., 2018. Towards a Holarctic synthesis of peatland testate amoeba ecology: development of a new continental-scale palaeohydrological transfer function for North America and comparison to European data. Quat. Sci. Rev. 201, 483–500.

Arlen-Pouliot, Y., Bhiry, N., 2005. Palaeoecology of a palsa and a filled thermokarst pond in a permafrost peatland, subarctic Québec, Canada. Holocene 15, 408–419.

Bakke, J., Lie, Ø., Dahl, S.O., Nesje, A., Bjune, A.E., 2008. Strength and spatial patterns of the Holocene wintertime westerlies in the NE Atlantic region. Global Planet. Change 60, 28–41.

Barber, K.E., Chambers, F.M., Maddy, D., Stoneman, R., Brew, J.S., 1994. A sensitive high-resolution record of late Holocene climatic change from a raised bog in northern England. Holocene 4, 198–205.

Belyea, L.R., 2009. Nonlinear dynamics of peatlands and potential feedbacks on the climate system. In: Baird, A.J., Belyea, L.R., Comas, X., Reeve, A., Slater, L.D. (Eds.), Carbon Cycling in Northern Peatlands. American Geophysical Union, Washington, pp. 5–18.

Bergeron, Y., Gauthier, S., Flannigan, M., Kafka, V., 2004. Fire regimes at the transition between mixedwood and coniferous boreal forest in northwestern Quebec. Ecology 85 (7), 1916–1932.

Blaauw, M., Christen, J.A., 2011. Flexible paleoclimate age-depth models using an autoregressive gamma process. Bayesian Analysis 6, 457–474.

Blundell, A., Hughes, P.D.M., Chambers, F.M., 2018. An 8000-year multi-proxy peat-based palaeoclimate record from Newfoundland: evidence of coherent changes in bog surface wetness and ocean circulation. Holocene 28, 791–805.

Booth, R.K., 2008. Testate amoebae as proxies for mean annual water-table depth in *Sphagnum*-dominated peatlands of North America. J. Quat. Sci. 23, 43–57.

Booth, R.K., Notaro, M., Jackson, S.T., Kutzbach, J.E., 2006. Widespread drought episodes in the western Great Lakes region during the past 2000 years: geographic extent and potential mechanisms. Earth Planet Sci. Lett. 242, 415–427.

Booth, R.K., Lamentowicz, M., Charman, D.J., 2010. Preparation and analysis of testate amoebae in peatland palaeoenvironmental studies. Mires Peat 7, 17.

Booth, R.K., Jackson, S.T., Sousa, V.A., Sullivan, M.E., Minckley, T.A., Clifford, M.J., 2012. Multi-decadal drought and amplified moisture variability drove rapid forest community change in a humid region. Ecology 93, 219–226.

Bruce, J.P., 2011. Climate Change Information for Adaption. Institute for Catastrophic Loss Reduction Report.

Chang, E.K.M., Ma, C.-G., Zheng, C., Yau, A.M.W., 2016. Observed and projected decrease in Northern Hemisphere extratropical cyclone activity in summer and its impacts on maximum temperature. Geophys. Res. Lett. 43, 2200–2208.

Charman, D.J., 2007. Summer water deficit variability controls on peatland water-table changes: implications for Holocene palaeoclimate reconstructions. Holocene 17, 217–227.

Charman, D.J., Hendon, D., Woodland, W.A., 2000. The Identification of Testate Amoebae (Protozoa: Rhizopoda) in Peats. Quaternary Research Association, London.

Charman, D.J., Barber, K.E., Blaauw, M., Langdon, P.G., Mauquoy, D., Daley, T.J., Hughes, P.D.M., Karofeld, E., 2009. Climate drivers for peatland palaeoclimate records. Quat. Sci. Rev. 28, 1811–1819.

Charman, D.J., Amesbury, M.J., Hinchliffe, W., Hughes, P.D.M., Mallon, G., Blake, W.H., Daley, T.J., Gallego-Sala, A.V., Mauquoy, D., 2015. Drivers of Holocene peatland carbon accumulation across a climate gradient in northeastern North America. Quat. Sci. Rev. 121, 110–119.

Clifford, M.J., Booth, R.K., 2013. Increased probability of fire during late Holocene droughts in northern New England. Climatic Change 119, 693–704.

Clifford, M.J., Booth, R.K., 2015. Late-Holocene drought and fire drove a widespread change in forest community composition in eastern North America. Holocene 25 (7), 1102–1110.

Coats, S., Smerdon, J.E., Cook, B.I., Seager, R., Cook, E.R., Anchukaitis, K.J., 2016. Internal ocean-atmosphere variability drives megadroughts in Western North

America. Geophys. Res. Lett. 43, 9886–9894.
Colle, B.A., Zhang, Z., Lombardo, K., Liu, P., Chang, E., Zhang, M., 2013. Historical evaluation and future prediction in Eastern North America and western Atlantic extratropical cyclones in the CMIP5 models during the cool season. J. Clim. 26, 6882–6903.
Cook, E.R., Seager Jr., R., Vose, R.S., Herweijer, C., Woodhouse, C., 2010. Mega-droughts in North America: placing IPCC projections of hydroclimatic change in a long-term palaeoclimate context. J. Quat. Sci. 25, 48–61.
Cook, B.I., Cook, E.R., Anchukaitis, K.J., Seager, R., Miller, R.L., 2011. Forced and unforced variability of twentieth century North American droughts and pluvials. Clim. Dynam. 37 (5–6), 1097–1110.
Cook, B.I., Cook, E.R., Smerdon, J.E., Seager, R., Williams, A.P., Coats, S., Stahle, D.W., Villanueva Díaz, J., 2016. North American megadroughts in the Common Era: reconstructions and simulations. Wiley Interdisciplinary Reviews: Climate Change 7 (3), 411–432.
Cronin, T.M., Hayo, K., Thunell, R.C., Dwyer, G.S., Saenger, C., Willard, D.A., 2010. The Medieval Climate Anomaly and Little Ice Age in Chesapeake Bay and the North Atlantic Ocean. Palaeogeogr. Palaeoclimatol. Palaeoecol. 297, 299–310.
Daley, T.J., Barber, K.E., Hughes, P.D.M., Loader, N.J., Leuenberger, M., Street-Perrott, F.A., 2016. The 8.2-ka BP event in north-eastern North America: first combined oxygen and hydrogen isotopic data from peat in Newfoundland. J. Quat. Sci. 31, 416–425.
Dieffenbacher-Krall, A.C., Nurse, A.M., 2005. Late-glacial and Holocene record of lake levels of mathews pond and whitehead lake, northern Maine, USA. J. Paleolimnol. 34, 283–310.
Dong, B., Sutton, R.T., Woollings, T., Hodges, K., 2013. Variability of the North Atlantic summer storm track: mechanisms and impacts on European climate. Environ. Res. Lett. 8, 034037.
D'Arrigo, R., Wilson, R., Jacoby, G., 2006. On the long-term context for late twentieth century warming. J. Geophys. Res. Atmos. 111.
Fillion, M.-E., Bhiry, N., Touazi, M., 2014. Differential development of two Palsa fields in a peatland located near Whapmagoostui-Kuujjuarapik, Northern Québec, Canada. Arctic Antarct. Alpine Res. 46, 40–54.
Gajewski, K., 1988. Late Holocene climate changes in eastern North America estimated from pollen data. Quat. Res. 29, 255–262.
Garneau, M., van Bellen, S., Magnan, G., Beaulieu-Audy, V., Lamarre, A., Asnong, H., 2014. Holocene carbon dynamics of boreal and subarctic peatlands from Québec, Canada. Holocene 24 (9), 1043–1053.
Gennaretti, F., Arseneault, D., Nicault, A., Perreault, L., Bégin, Y., 2014. Volcano-induced regime shifts in millennial tree-ring chronologies from northeastern North America. Proc. Natl. Acad. Sci. U.S.A. 111 (28), 10077–10082.
Graham, N.E., Ammann, C.M., Fleitmann, D., Cobb, K.M., Luterbacher, J., 2010. Support for global climate reorganization during the "Medieval Climate Anomaly". Clim. Dynam. 37, 1217–1245.
Grove, J.M., 1988. The Little Ice Age. Routledge, London, p. 498.
Hendon, D., Charman, D.J., 1997. The preparation of testate amoebae (Protozoa: rhizopoda) samples from peat. Holocene 7, 199–205.
Hogg, E.H., 1997. Temporal scaling of moisture and the forest-grassland boundary in western Canada. Agric. For. Meteorol. 84, 115–122.
Holmquist, J.R., Booth, R.K., MacDonald, G.M., 2016. Boreal peatland water table depth and carbon accumulation during the Holocene Thermal Maximum, Roman Warm Period, and Medieval Climate Anomaly. Palaeogeogr. Palaeoclimatol. Palaeoecol. 444, 15–27.
Houle, D., Moore, J.-D., Provencher, J., 2007. Ice bridges on the St. Lawrence river as an index of winter severity from 1620 to 1910. J. Clim. 20 (4), 757–764.
Hughes, P.D.M., Blundell, A., Charman, D.J., Bartlett, S., Daniell, J.R.G., Wojatschke, A., Chambers, F.M., 2006. An 8500 cal. year multi-proxy climate record from a bog in eastern Newfoundland: contributions of meltwater discharge and solar forcing. Quat. Sci. Rev. 25, 1208–1227.
Hutchinson, M.F., 2004. Anusplin Version 4.3. Centre for Resource and Environmental Studies. Aust. Natl. Univ, Canberra, ACT.
Ineson, S., Scaife, A.A., Knight, J.R., Manners, J.C., Dunstone, N.J., Gray, L.J., Haigh, J.D., 2011. Solar forcing of winter climate variability in the Northern Hemisphere. Nat. Geosci. 4, 753–757.
Jansen, E., Overpeck, J., Briffa, K.R., Duplessy, J.-C., Joos, F., Masson-Delmotte, V., Olago, D., Otto-Bliesner, B., Peltier, W.R., Rahmstorf, S., Ramesh, R., Raynaud, D., Rind, D., Solomina, O., Villalba, R., Zhang, D., 2007. Palaeoclimate. In: Solomon, S., Qin, D., Manning, M., Chen, Z., Marquis, M., Averyt, K.B., Tignor, M., Miller, H.L. (Eds.), Climate Change 2007: the Physical Science Basis. Contribution of Working Group I to the Fourth Assessment Report of the Intergovernmental Panel on Climate Change. Cambridge University Press, pp. 433–497.
Juggins, S., 2013. Quantitative reconstructions in palaeolimnology: new paradigm or sick science? Quat. Sci. Rev. 64, 20–32.
Knutson, T.R., Sirutis, J.J., Zhao, M., Tuleya, R.E., Bender, M., Vecchi, G.A., Villarini, G., Chavas, D., 2015. Global projections of intense tropical cyclone activity for the late twenty-first century from dynamical downscaling of CMIP5/rcp4.5 scenarios. J. Clim. 28 (18), 7203–7224.
Kottek, M., Grieser, J., Beck, C., Rudolf, B., Rubel, F., 2006. World Map of the Köppen-Geiger climate classification updated. Meterologische Zeitschrift 15 (3), 259–263.
Kunkel, K.E., Karl, T.R., Easterling, D.R., Redmond, K., Young, J., Yin, X., Hennon, P., 2013. Probable maximum precipitation and climate change. Geophys. Res. Lett. 40, 1402–1408.
Ladd, M., Viau, A., Way, R., Gajewski, K., Sawada, M., 2018. Variations in precipitation in North America during the past 2000 years. Holocene 28 (4), 667–675.
Lafontaine-Boyer, K., Gajewski, K., 2014. Vegetation dynamics in relation to late Holocene climate variability and disturbance, Outaouais, Quebec, Canada. Holocene 24, 1515–1526.
Lamarre, A., Magnan, G., Garneau, M., Boucher, É., 2013. A testate amoeba-based transfer function for paleohydrological reconstruction from boreal and subarctic peatlands in northeastern Canada. Quat. Int. 306, 88–96.
Lamb, H.H., 1977. Climate: Present, Past and Future. Methuen, London.
Linderholm, H., Folland, C., 2017. Summer North Atlantic Oscillation (SNAO) variability on decadal to palaeoclimate time scales. Past Global Changes Magazine 25, 57–60. https://doi.org/10.22498/pages.25.1.57.
Loisel, J., MacDonald, G.M., Thomson, M.J., 2017. Little Ice Age climatic erraticism as an analogue for future enhanced hydroclimatic variability across the American Southwest. PloS One 12 (10), e0186282.
Lund, D.C., Lynch-Stieglitz, J., Curry, W.B., 2006. Gulf Stream density structure and transport during the past millennium. Nature 444, 601–604.
Lüning, S., Galka, M., Vahrenholt, F., 2017. Warming and cooling: the medieval climate anomaly in africa and arabia. Paleooceanography 32, 1219–1235.
Mackay, H., 2016. Testing Peatland Carbon Responses to Late Holocene Climate Change in Eastern North America. PhD Thesis. University of Southampton, School of Geography, p. 476. https://eprints.soton.ac.uk/386576/.
Mackay, H., Hughes, P.D.M., Jensen, B.J.L., Langdon, P.G., Pyne-O'Donnell, S.D.F., Plunkett, G., Froese, D.G., Coulter, S., Gardner, J.E., 2016. A mid to late Holocene cryptotephra framework from eastern North America. Quat. Sci. Rev. 132, 101–113.
Magnan, G., Garneau, M., 2014. Evaluating long-term regional climate variability in the maritime region of the St. Lawrence North Shore (eastern Canada) using a multi-site comparison of peat-based paleohydrological records. J. Quat. Sci. 29, 209–220.
Magnan, G., van Bellen, S., Davies, L., Froese, D., Garneau, M., Mullan-Boudreau, G., Zaccone, C., Shotyk, W., 2018. Impact of the Little Ice Age cooling and 20th century climate change on peatland vegetation dynamics in central and northern Alberta using a multi-proxy approach and high-resolution peat chronologies. Quat. Sci. Rev. 185, 230–243.
Mann, M.E., Zhang, Z., Hughes, M.K., Bradley, R.S., Miller, S.K., Rutherford, S., Ni, F., 2008. Proxy-based reconstructions of hemispheric and global surface temperature variations over the past two millennia. Proc. Natl. Acad. Sci. U.S.A. 105, 13252–13257.
Mann, M.E., Zhang, Z., Rutherford, S., Bradley, R.S., Hughes, M.K., Shindell, D., Ammann, C., Faluvegi, G., Ni, F., 2009. Global signatures and dynamical origins of the Little Ice Age and Medieval Climate Anomaly. Science 326, 1256–1260.
Mann, M.E., Steinman, B.A., Miller, S.K., 2020. Absence of internal multidecadal and interdecadal oscillation in climate model simulations. Nat. Commun. 11, 49.
Marlon, J.R., Pederson, N., Nolan, C., Goring, S., Shuman, B., Robertson, A., Booth, R., Bartlein, P.J., Berke, M.A., Clifford, M., Cook, E., Dieffenbacher-Krall, A., Dietze, M.A., Hessl, A., Hubeny, J.B., Jackson, S.T., Marsicek, J., McLachlan, J., Mock, C.J., Moore, D.J.P., Nichols, J., Peteet, D., Schaefer, K., Trouet, V., Umbanhowar, C., Williams, J.W., Yu, Z., 2017. Climatic history of the northeastern United States during the past 3000 years. Clim. Past 13, 1355–1379.
Martin-Puertas, C., Matthes, K., Brauer, A., Muscheler, R., Hansen, F., Petrick, C., Aldahan, A., Possnert, G., Van Geel, B., 2012. Regional atmospheric circulation shifts induced by a grand solar minimum. Nat. Geosci. 5, 397–401.
McKenney, D.W., Hutchinson, M.F., Papadopol, P., Lawrence, K., Pedlar, J., Campbell, K., Milewska, E., Hopkinson, R.F., Price, D., Owen, T., 2011. Customized spatial climate models for North America. Bull. Am. Meteorol. Soc. 92, 1611–1622.
Mitchell, E.A.D., Charman, D.J., Warner, B.G., 2008. Testate amoebae analysis in ecological and paleoecological studies of wetlands: past, present and future. Biodivers. Conserv. 17, 2115–2137.
Moffa-Sánchez, P., Moreno-Chamarro, E., Reynolds, D.J., Ortega, P., Cunningham, L., Swingedouw, D., Amrhein, D.E., Halfar, J., Jonkers, L., Jungclaus, J.H., Perner, K., Wanamaker, A., Yeager, S., 2019. Variability in the northern North Atlantic and Arctic Oceans across the last two millennia: a review. Paleoceanography and Paleoclimatology 34, 1399–1436.
Morris, P.J., Baird, A.J., Young, D.M., Swindles, G.T., 2015. Untangling climate signals from autogenic changes in long-term peatland development. Geophys. Res. Lett. 42, 10788–10797.
Naulier, M., Savard, M.M., Bégin, C., Gennaretti, F., Arseneault, D., Marion, J., Nicault, A., Bégin, Y., 2015. A millennial summer temperature reconstruction for northeastern Canada using oxygen isotopes in subfossil trees. Clim. Past 11 (9), 1153–1164.
Neil, K., Gajewski, K., 2017. Impacts of late-Holocene climate variability and watershed-lake interactions on diatom communities in Lac Brûlé, Québec. Ecosphere 8, e01886.
Neukom, R., Schurer, A.P., Steiger, N.J., Hegerl, G.C., 2018. Possible causes of data model discrepancy in the temperature history of the last Millennium. Sci. Rep. 8, 7572.
Newby, P.E., Shuman, B.N., Donnelly, J.P., Karnauskas, K.B., Marsicek, J., 2014. Centennial-to-millennial hydrologic trends and variability along the North Atlantic coast, USA, during the Holocene. Geophys. Res. Lett. 41, GL060183.
Nichols, J.E., Huang, Y., 2012. Hydroclimate of the northeastern United States is highly sensitive to solar forcing. Geophys. Res. Lett. 39.
Oswald, W.W., Foster, D.R., 2011. A record of late-Holocene environmental change from southern New England, USA. Quat. Res. 76, 314–318.
Paquette, N., Gajewski, K., 2013. Climatic change causes abrupt changes in forest composition, inferred from a high-resolution pollen record, southwestern

Québec, Canada. Quat. Sci. Rev. 75, 169–180.
Payne, R.J., Mitchell, E.A., 2009. How many is enough? Determining optimal count totals for ecological and palaeoecological studies of testate amoebae. J. Paleolimnol. 42, 483–495.
Peros, M., Chan, K., Magnan, G., Ponsford, L., Carroll, J., McCloskey, T., 2016. A 9600-year record of water table depth, vegetation and fire inferred from a raised peat bog, Prince Edward Island, Canadian Maritimes. J. Quat. Sci. 31, 512–525.
Pfahl, S., Schwierz, C., Croci-Maspoli, M., Grams, C.M., Wernli, H., 2015. Importance of latent heat release in ascending air streams for atmospheric blocking. Nat. Geosci. 8, 610–614.
Piilo, S.R., Zhang, H., Garneau, M., Gallego-Sala, A., Amesbury, M.J., Väliranta, M.M., 2019. Recent peat and carbon accumulation following the Little Ice Age in northwestern Québec, Canada. Environ. Res. Lett. 14, 075002.
Rahmstorf, S., Box, J., Feulner, G., Mann, M., Robinson, A., Rutherford, S., Schaffernicht, E., 2015. Exceptional twentieth-Century slowdown in Atlantic Ocean overturning circulation. Nat. Clim. Change 5, 475–480.
Shuman, B.N., Routson, C., McKay, N., Fritz, S., Kaufman, D., Kirby, M.E., Nolan, C., Pederson, G.T., St-Jacques, J.-M., 2018. Placing the Common Era in a Holocene context: millennial to centennial patterns and trends in the hydroclimate of North America over the past 2000 years. Clim. Past 14, 665–686.
Steiger, N.J., Smerdon, J.E., Cook, B.I., Seager, R., Williams, A.P., Cook, E.R., 2018. A reconstruction of global hydroclimate and dynamical variables over the Common Era. Scientific data 5, 180086.
Steiger, N.J., Smerdon, J.E., Cook, B.I., Seager, R., Williams, A.P., Cook, E.R., 2019. Oceanic and radiative forcing of medieval megadroughts in the American Southwest. Science Advances 5 (7), eaax008.
Sullivan, M.E., Booth, R.K., 2011. The potential influence of short-term environmental variability on the composition of testate amoeba communities in Sphagnum peatlands. Microb. Ecol. 62, 80–93.
Sutton, R., Dong, B., 2012. Atlantic Ocean influence on a shift in European climate in the 1990s. Nat. Geosci. 5, 788–792.
Swindles, G.T., Morris, P.J., Baird, A.J., Blaauw, M., Plunkett, G., 2012. Ecohydrological feedbacks confound peat-based climate reconstructions. Geophys. Res. Lett. 39.
Swindles, G.T., Holden, J., Raby, C.L., Turner, T.E., Blundell, A., Charman, D.J., Walle Menberu, M., Kløve, B., 2015. Testing peatland water-table depth transfer functions using high-resolution hydrological monitoring data. Quat. Sci. Rev. 120, 107–117.
Thibodeau, B., de Vernal, A., Hillaire-Marcel, C., Mucci, A., 2010. Twentieth century warming in deep waters of the Gulf of St. Lawrence: a unique feature of the last millennium. Geophys. Res. Lett. 37, L17604.
Thornalley, D.J.R., Oppo, D.W., Ortega, P., Robson, J.I., Brierley, C.M., Davis, R., Hall, I.R., Moffa-Sanchez, P., Rose, N.L., Spooner, P.T., Yashayaev, I., Keigwin, L.D., 2018. Anomalously weak Labrador Sea convection and Atlantic overturning during the past 150 years. Nature 556, 227–230.
Ting, M., Kossin, J.P., Camargo, S.J., Li, C., 2019. Past and future hurricane intensity change along the U.S. East coast. Sci. Rep. 9, 7795.
Tröels-Smith, J., 1955. Characterisation of unconsolidated sediments. Danmarks geologiska undersögelse IV. Reakke 3, 1–73.
Trouet, V., Esper, J., Graham, N.E., Baker, A., Scourse, J.D., Frank, D.C., 2009. Persistent positive North Atlantic oscillation mode dominated the Medieval Climate Anomaly. Science 324, 78–80.
Turner, T.E., Swindles, G.T., Charman, D.J., Blundell, A., 2013. Comparing regional and supra-regional transfer functions for palaeohydrological reconstruction from Holocene peatlands. Palaeogeogr. Palaeoclimatol. Palaeoecol. 369, 395–408.
Van Bellen, S., Garneau, M., Booth, R.K., 2011. Holocene carbon accumulation rates from three ombrotrophic peatlands in boreal Quebec, Canada: impact of climate-driven ecohydrological change. Holocene 21 (8), 1217–1231.
van Bellen, S., Magnan, G., Davies, L., Froese, D., Mullan-Boudreau, G., Zaccone, C., Shotyk, W., 2018. Testate amoeba records indicate regional 20th-century lowering of water tables in ombrotrophic peatlands in central-northern Alberta, Canada. Global Change Biol. 24 (7), 2758–2774.
Viau, A.E., Ladd, M., Gajewski, K., 2012. The climate of North America during the past 2000 years reconstructed from pollen data. Global Planet. Change 84–85, 75–83.
Woodland, A., Charman, D.J., Sims, P.C., 1998. Quantitative estimates of water tables and soil moisture in Holocene peatlands from testate amoebae. Holocene 8, 261–273.
Wuebbles, D.J., Fahey, D.W., Hibbard, K.A., DeAngelo, B., Doherty, S., Hayhoe, K., Horton, R., Kossin, J.P., Taylor, P.C., Waple, A.M., Weaver, C.P., 2017. In: Wuebbles, D.J., Fahey, D.W., Hibbard, K.A., Dokken, D.J., Stewart, B.C., Maycock, T.K. (Eds.), Executive Summary of the Climate Science Special Report: Fourth National Climate Assessment, vol. I. U.S. Global Change Research Program, Washington, DC, USA, p. 26.
Yu, Z., Vitt, D.H., Campbell, I.D., Apps, M.J., 2003. Understanding Holocene peat accumulation pattern of continental fens in western Canada. Can. J. Bot. 81, 267–282.